A Readout System for a TPC Detector

by

Joshua Michael Thompson

Submitted to the Department of Physics
in partial fulfillment of the requirements for the degree of

Bachelor of Science in Physics

at the

MASSACHUSETTS INSTITUTE OF TECHNOLOGY

June 2002

Author .....
Department of Physics
May 10, 2002

Certified by .....
Ulrich J. Becker
Professor, Department of Physics
Thesis Supervisor

Accepted by .....
David Pritchard
Senior Thesis Coordinator, Department of Physics

A Readout System for a TPC Detector

by

Joshua Michael Thompson

Submitted to the Department of Physics
on May 10, 2002, in partial fulfillment of the
requirements for the degree of
Bachelor of Science in Physics

Abstract

A mini-TPC was configured for readout via CAMAC to a PC running LabView. Tracks were reconstructed and ranges determined for 5.5 MeV alpha particles. Using alpha particle signals in Argon:CH_4 (90:10)%, the wire pulse charge and risetime were measured as a function of drift field. Triggering on scintillators, 3-d cosmic ray tracks were obtained and reconstructed using the pads (x-y) and wires (z). By finding the distributions of the residuals of the fit tracks, the detector's position resolution was determined.

Thesis Supervisor: Ulrich J. Becker
Title: Professor, Department of Physics

Acknowledgments

I would like to thank Prof. Ulrich Becker for making this thesis possible. Thanks also go to Profs. Peter Fisher, Kate Scholberg, and Sekazi Mtingwa for their input and support, and to the students of Building 44, Kasey Ensslin, Teresa Fazio, Kendall McConnel, Reyco Henning, Gianpaolo Carosi, Bilge Demirköz, and Ben Monreal. Vladimir Koutsenko provided technical assistance.

Contents

1 Drift chambers—purpose and principles **9**

1.1 The time projection principle 10

1.2 Existing TPCs 10

2 Apparatus and methodology **12**

2.1 The Test TPC at MIT 12

2.1.1 Configuration 12

2.1.2 Gas selection 13

2.1.3 Operating voltages 16

2.1.4 On-board electronics 16

2.2 Readout 17

2.2.1 Charge distribution on pads 17

2.2.2 Wire readout 18

3 Measurements **19**

3.1 Alpha source 19

3.1.1 Triggering 19

3.1.2 Measurements of Signal Shape as a function of Drift Field . . 20

3.2 Cosmic rays 22

3.2.1 Triggering 22

3.2.2 Scintillator Setup 22

3.3 Recording procedure in TPC 24

3.3.1 Calibrations and pedestal correction 24

3.3.2 Data readout 27

4 Data and analysis **30**

4.1 Alpha particles 30

4.1.1 Range determination 33

4.1.2 Measurements as a function of drift field 38

4.2 3-D tracks of cosmic rays 40

4.2.1 x, y reconstruction with pads 42

4.2.2 z reconstruction with wires 43

4.2.3 Track resolution 43

5 Summary **47**

A Data collection instructions **48**

A.1 Wire-Based Trigger 48

A.2 Scintillator-Based Trigger 50

List of Figures

1-1 Particle tracking using the time projection principle. The pads allow a 2-d reconstruction of the particle track. The z coordinate is obtained from the drift distance, as measured by the timing of the signals on the wires. 11

2-1 The experimental setup in operation. From left, the NIM and CAMAC crates, the scope (showing an alpha event), and the TPC. 13

2-2 View of TPC with top removed, showing exposed field cage. Connectors for pad readout are visible on the right side of the image. Several of the Lemo wires leading to the oscilloscope are also visible. 14

2-3 Sense wires seen from above the pad plane. 14

2-4 Side view of the amplification gap. The field cage has a total of 18 layers for a height of 144 mm. 15

2-5 The drift velocity of Ar:CH_4 90:10% (P10) as a function of drift field. [10, 4] 15

3-1 Electronics and connections for alpha particle readout using a sense wire trigger. 21

3-2 The x-z plane of the TPC, showing the ends of the sense wires. The identification numbers for wire pairs and the corresponding oscilloscope channels for alpha data collection are shown. The wire pairs used for cosmic ray events are shown in red. For cosmics, up is to the right. . 21

3-3 Electronics and connections for cosmic ray readout using a pair of scintillators (S1 and S2) as a trigger. 23

3-4 View of the y-z plane of the TPC, with projected scintillator positions. 25
3-5 View of the x-y plane of the TPC, with initial scintillator positions. The blue line shows how a cosmic particle would travel through the TPC and both scintillators, creating a track to be read out on the pads. 26
3-6 View of the y-z plane of the TPC, showing the top scintillator (S1) in its initial position. 28
3-7 View of the x-y plane of the TPC, with initial scintillator positions. . 29

4-1 Event rates as measured by a scaler connected to the TPC's discriminated wire outputs. The Channel labels refer to oscilloscope channels receiving signals from a wire doublet. 31
4-2 Oscilloscope output of a sample alpha particle event. The trigger for this event came from the wire on oscilloscope channel 4. 31
4-3 Pad output of the sample alpha particle event shown in Fig. 4-2. The area of each filled rectangle is proportional to the charge on the pad, normalized to the maximum charge Q_{max}. The points are the centers of charge calculated using eq. 4.6, with the best fit line shown in green. The purple square is the location of the alpha source, and the dashed lines outline the active readout area. For a description of the fitting procedure, see Section 4.2.1. 32
4-4 The crossing point is the location of the alpha source, as determined by the crossing point of these tracks. The colors of the tracks represent the trigger wire. Green=Wire 8, Blue=Wire 9, Magenta=Wire 10 . . 33
4-5 The general form of dE/dx as a function of distance from the particle source. [12] 34
4-6 Range data collected using several different wires as trigger. For a key to the wire numbers, see Fig. 3-2. For each wire, the number of counts in each bin is normalized to the total number of counts in the data set. The data sets are then summed as indicated by the legend. 36

4-7 An event taken at 420 Torr. Note that the particle traveled in a path long enough that its charge distribution is cut off at the edge of the detected region of the pads. (The bottom three pads of each row were not being read out.) 37
4-8 Reduced pressure: Oscilloscope data to accompany Figure 4-7. Scale: 0.1 μs/div, 20 mV/div 37
4-9 Alpha particle wire pulses at varying drift fields. 38
4-10 Average integrated wire charge generated by the alpha source. 39
4-11 Diffusion in Argon:CH_4 (90:10)% as a function of drift field. Points are derived from the derivative of the rising side of alpha event wire signals and the curve is generated by Magboltz. 41
4-12 Track of a cosmic ray. The dashed lines outline the active readout area. The direction of the ceiling is to the right on the graph. 42
4-13 Wire signals to accompany the track shown in Figure 4-12. The scope channels were connected to evenly spaced wires along the TPC (see Figure 3-2). The plot on the right shows the best fit of these signals. The measured time corresponds to the drift distance in the z direction. 44
4-14 Residuals from pad data. Aggregate data from 82 cosmic ray events. Gaussian fit parameters: $\sigma = 1.3$ mm, mean $= 0.24$ mm 45
4-15 Residuals from wire data. Aggregate data from 18 cosmic ray events. Gaussian fit parameters: $\sigma = 0.8$ mm, mean $= 0.10$ mm 46

Chapter 1

Drift chambers—purpose and principles

Drift chambers are among the most common particle detectors. They are particularly useful for reconstruction of a particle's path, and can also measure its energy loss. The particle path in a magnetic field allows for the determination of particle momentum. The latter measurement is used for particle identification.

The drift chamber is a multi-wire proportional chamber (MWPC) with an added gas volume. In the path of an ionizing particle, electrons are freed from gas molecules. With a constant electric field over the gas volume, the freed electrons drift at constant velocity toward the MWPC. In the vicinity of the signal wires, which are at a positive high-voltage, the drifting electrons rapidly accelerate and gain energy. They then cause secondary ionizations, which in turn cause tertiary ionizations, and so on. The process multiplies into an "avalanche" of charge. The final charge deposited on the wire is proportional to the initial number of drifting electrons with an amplification on the order of 10^4.

A measurement of the time from a particle event to the detection of a signal on the wire gives information on how far the electrons had to drift. Often, multiple drift chambers are stacked in order to determine a particle track completely. To reconstruct additional dimensions of a track, drift chambers sometimes employ layers of wires at crossing angles or techniques such as charge division. [12]

1.1 The time projection principle

A type of drift chamber known as a Time Projection Chamber (TPC) has gone into increasing use at major experiments, especially for central tracking systems. Proposed in the late 1970s, TPCs differ from standard drift chambers in that they typically have large detection volumes, have all of the drift volume on one side of the sense wires, and use cathode pads to supplement the sense wire readout. The pads are arranged in a grid, but need not be rectangular. Also, if a magnetic field is present, it is applied parallel to the drift field to reduce transverse diffusion. [13]

TPC operation is based on the time projection principle. Charge deposited on the signal wires induce charges on the cathode pads below the wires, creating a two-dimensional (x, y) projection of the particle track through the detector volume. $z = v_d t$, where t is the drift time and v_d is the constant drift velocity, yields the distance z from a sense wire to the particle track. The combination of the timing data with the track projection yields a complete 3-d picture of the particle track. It is this simplicity in track reconstruction combined with the ability to cover a large detection volume that make TPCs such attractive detectors. The time projection principle is illustrated in Figure 1-1.

1.2 Existing TPCs

The functionality of TPCs has been proven at several major experiments in recent years. Two of the four experiments at the Large Electron-Positron (LEP) collider at CERN, which ran for 12 years ending in 2000, featured TPCs. The DELPHI and ALEPH experiments both used TPCs as their primary detector for track reconstruction and also as a source of dE/dx information. [16, 1] An earlier e^+e^- collider at KEK, TRISTAN, employed a TPC for the same purposes in its TOPAZ detector. [9] The PEP4 detector at the SLAC PEP e^+e^- facility, which began data collection in 1982, also used a TPC. [6] All of these TPCs used mixtures of argon and methane as drift gases, with argon ranging from 80 to 91 percent of the total.

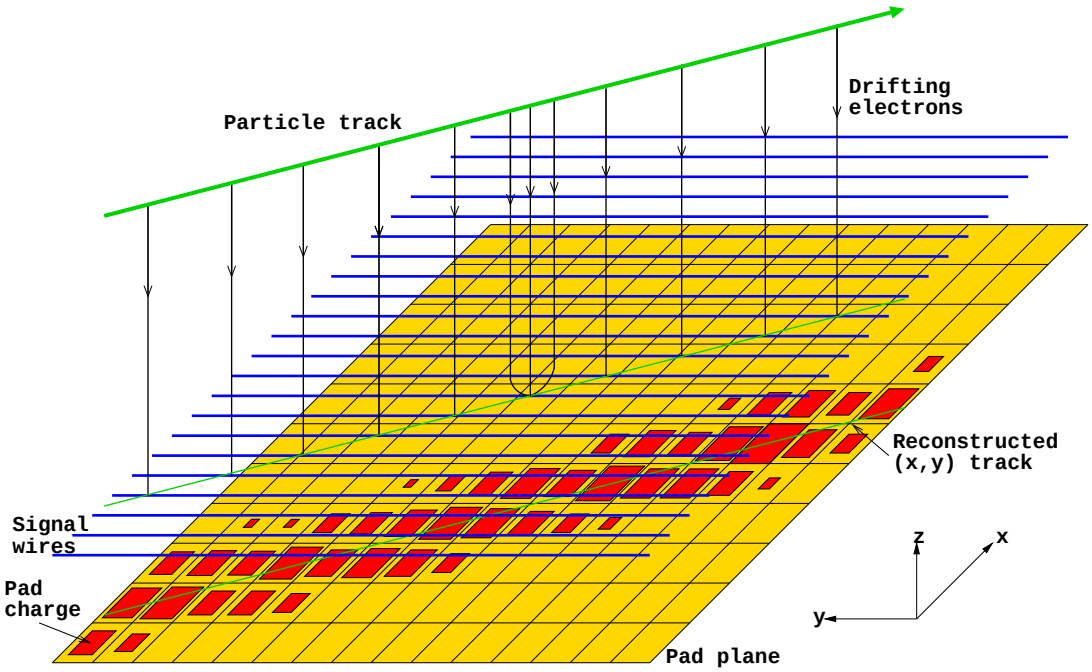

Figure 1-1: Particle tracking using the time projection principle. The pads allow a 2-d reconstruction of the particle track. The z coordinate is obtained from the drift distance, as measured by the timing of the signals on the wires.

TPCs have not been limited to lepton colliders. They have also proven useful for heavy ion collisions. The large number of particles created in these events make the straightforward tracking capabilities of TPCs very useful. The NA36 experiment at CERN SPS and the STAR detector at the Relativistic Heavy Ion Collider (RHIC) at Brookhaven both use TPCs. These detectors place emphasis on accurate track reconstruction and sacrifice the measurement of energy loss. [5, 7]

Several more TPCs are planned for experiments at future accelerators. ALICE, a heavy ion experiment to be built at the Large Hadron Collider (LHC) at CERN, will employ a TPC for tracking. [2] The TESLA linear collider, proposed for construction at DESY, will use a large TPC. The next generation of e^+e^- collider, TESLA will reach energies of 500 GeV and beyond. The proposed TPC is large, with a radius of 170 cm and a length of over 5 m. [3] Researchers developing the Next Linear Collider (NLC), a proposed accelerator for the United States, are also considering a TPC. [15]

Chapter 2

Apparatus and methodology

2.1 The Test TPC at MIT

A small TPC was built by Ulrich Becker and Vladimir Koutsenko, complete with on-board electronics. Figures 2-1 and 2-2 are external and internal views of the TPC. The features of this TPC are described here.

2.1.1 Configuration

Mechanical and gas setup

The TPC is an aluminum box with an approximate volume of 15 liters. See Figure 3-4 for detailed dimensions. The on-board electronics are mounted on an aluminum extension from the bottom of the box.

Connections are provided at the top of the TPC opposite the electronics and at the bottom of the TPC near the electronics for the entry and exit, respectively, of the chamber gas. Gas is supplied from a premixed gas bottle ("P10," see Section 2.1.2) through a copper pipe to a Swagelok quick-connector. This connector plugs into a plastic pipe connected to the TPC gas input, for a total length of approximately 2 m of 1/4 inch diameter pipe. The gas exit flows through a needle valve and into a 1.5 m long section of copper pipe. This pipe connects to flexible plastic tubing which vents to a hood through a bubbler.

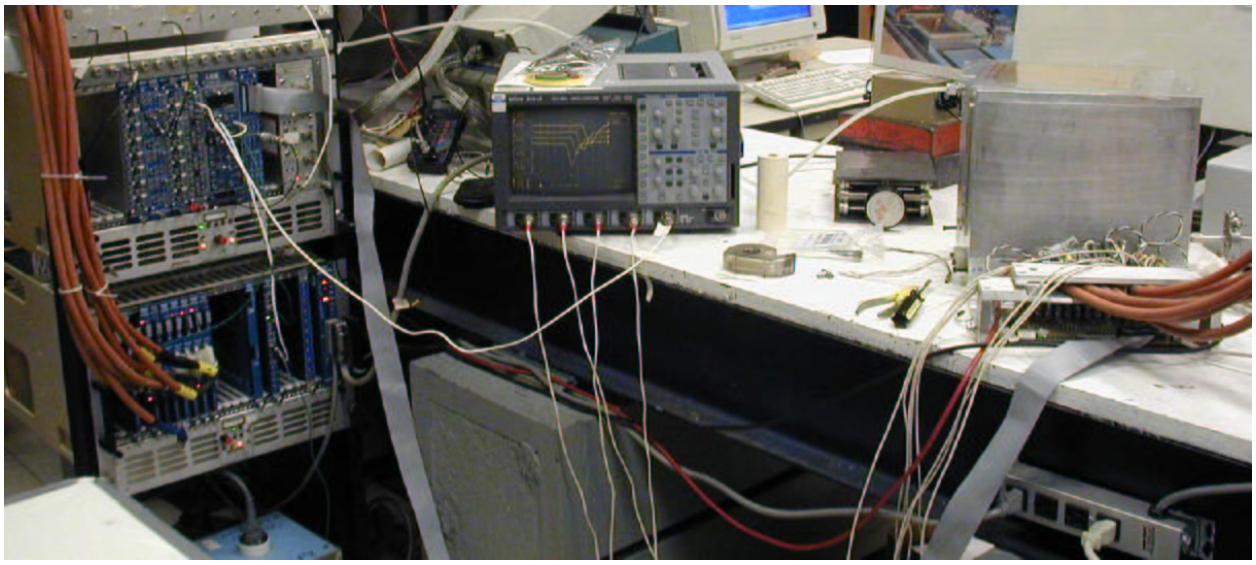

Figure 2-1: The experimental setup in operation. From left, the NIM and CAMAC crates, the scope (showing an alpha event), and the TPC.

Inside the TPC, the drift field is created by a copper cage of inside dimensions 15 cm by 19.5 cm. There are 18 layers spaced 8 mm apart for a total height of 144 mm. The cage layers are connected with 10 MΩ resistors to form a voltage divider. With the bottom at ground, applying a negative high voltage to the top of the cage creates an electric field pointing up, making electrons want to drift down.

Wires and pads

A grid of copper "pads," 6 mm by 12 mm each, sits on the bottom of the TPC. There are 16 pad rows (12 mm wide) and 24 pads in each row. The sense wires are strung above (6 mm) and parallel to each pad row. The wires have a 3 mm separation, meaning that 4 wires are strung over each pad row, as shown in Figure 2-3. Figure 2-4 shows the vertical dimensions of the amplification gap and the first layer of the field cage.

2.1.2 Gas selection

Several parameters must be considered when choosing a TPC drift gas. Because TPCs have large drift distances, the gas must have low diffusion to avoid degrading

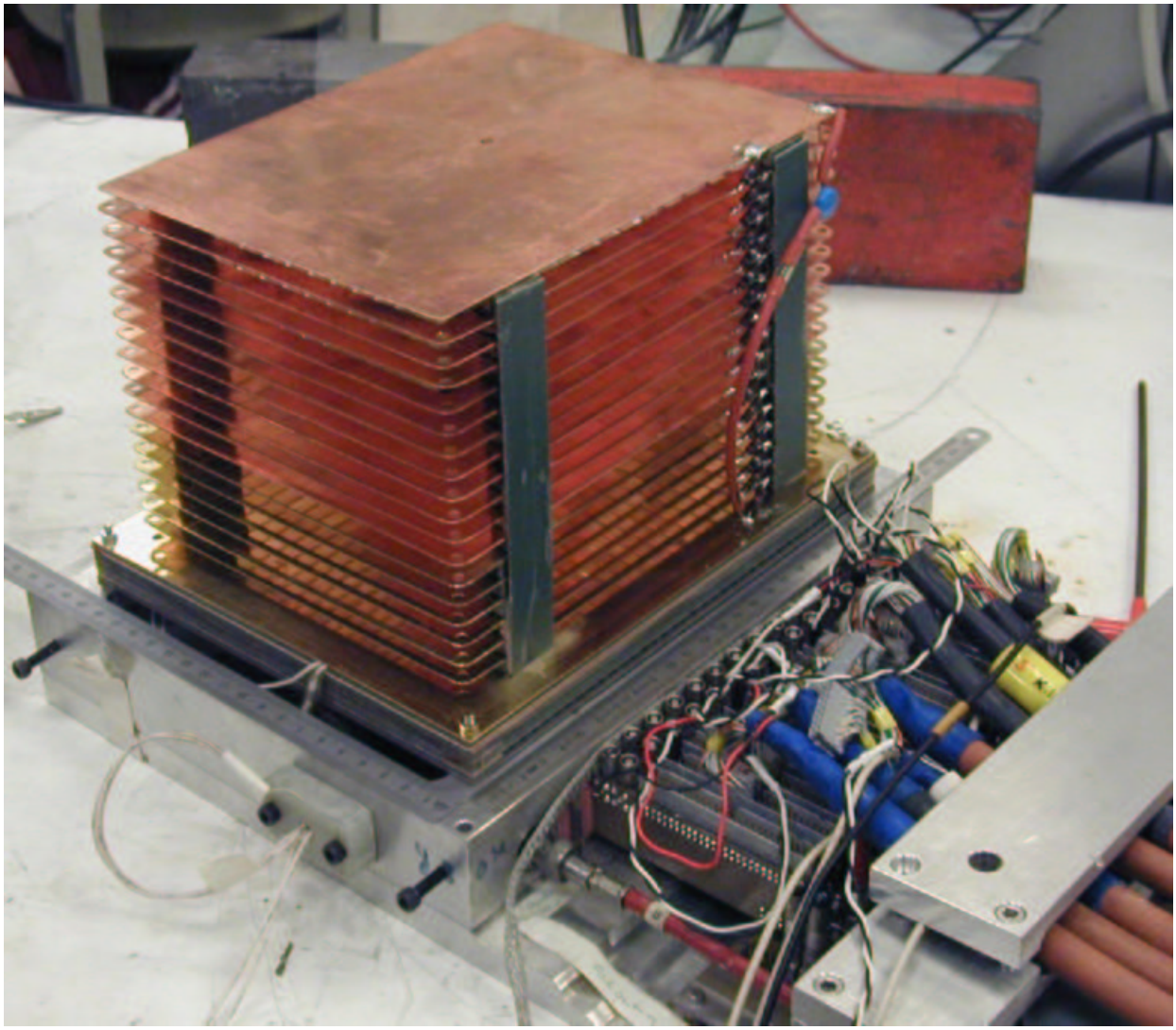

Figure 2-2: View of TPC with top removed, showing exposed field cage. Connectors for pad readout are visible on the right side of the image. Several of the Lemo wires leading to the oscilloscope are also visible.

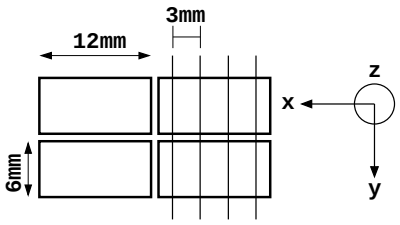

Figure 2-3: Sense wires seen from above the pad plane.

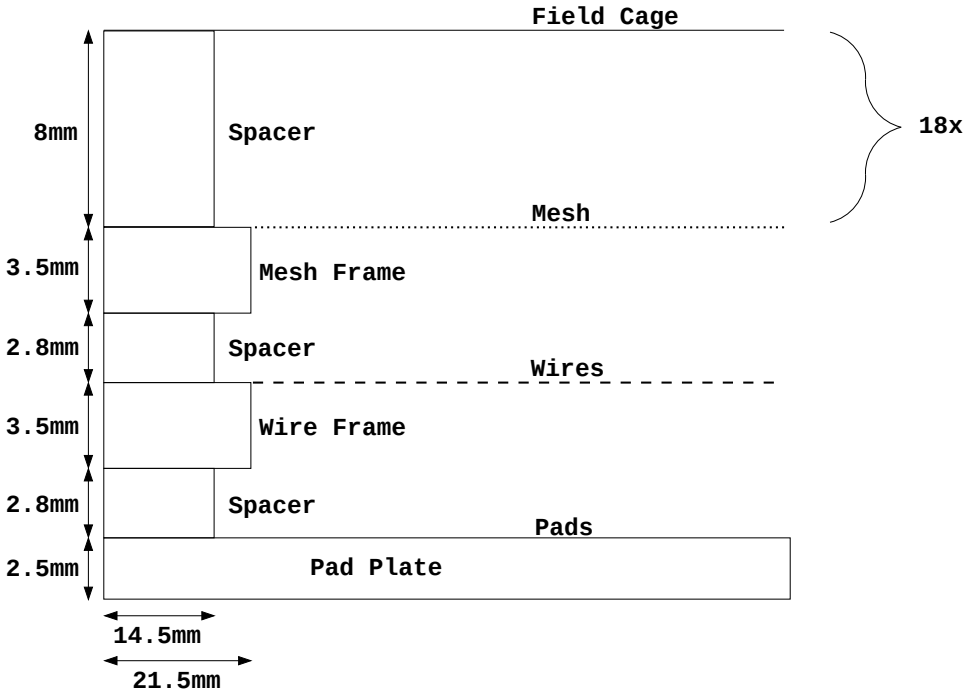

Figure 2-4: Side view of the amplification gap. The field cage has a total of 18 layers for a height of 144 mm.

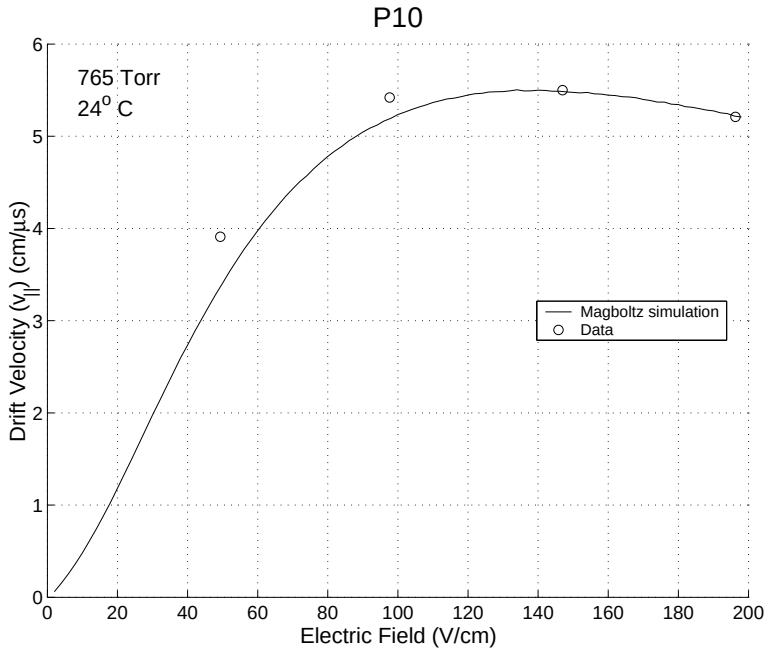

Figure 2-5: The drift velocity of Ar:CH_4 90:10% (P10) as a function of drift field. [10, 4]

the resolution. Desired drift velocity characteristics vary. Gases with slow drift velocities increase the resolution in the z-direction. [12] For the proposed TESLA TPC, however, a fast drift speed is desired to minimize the time before the TPC is cleared of electrons from an event. [3]

I looked for a gas with a low operating point ($E < 150$V/cm) to minimize the required drift voltage and high drift velocity (> 4cm/μs) to minimize drift time. Using the computer simulation software Magboltz, the drift velocity curves of a number of gas mixtures were compared. [4] We chose to use a mixture of Argon:Methane (90:10)% ("P10"). This mixture is inexpensive, ionizes heavily, and has a peak drift velocity at an achievable electric field. I found that introducing small percentages of additives such as CF_4 or CO_2 to the gas increased operating points to unacceptable levels. Increasing the ratio of argon to methane decreased the maximum drift velocity.

2.1.3 Operating voltages

The Magboltz simulation of the drift velocity of electrons in P10 as a function of electric field was confirmed with empirical data. [4, 10] The curve, shown in Figure 2-5, peaks at a field of approximately 135 V/cm. The base drift voltage, therefore, was 135V/cm $\times$ 14.4cm = 1940V. This field was varied significantly, however, for various tests.

The sense wires are operated at a positive voltage high enough to provide enough gain to give an adequate signal-to-noise ratio, but low enough to maintain stability (avoid sparking) and stay in the proportional gain region. This voltage ranged from approximately 1800 V to 2400 V, where every 80 volts approximately doubles the gain. The exact voltage used will be mentioned on a case-by-case basis.

2.1.4 On-board electronics

The TPC's wires are grouped into pairs of adjacent wires for readout. In other words, the four wires over each pad become two channels of readout. These paired wire signals are passed through current amplifiers and are output through Lemo

jacks. The wire signals are also discriminated into logic pulses and made available for readout at a pair of 2×17 pin outputs. The discriminator thresholds are set to 7 mV.

The pad signals are charge amplified. Each row of pad signals is made available for readout at a 2×25 pin output.

2.2 Readout

The system designed to perform the readout of the TPC's data is based around a Pentium III PC running Windows 2000. The data acquisition (DAQ) software was written using LabView 6.0, and interfaces with several pieces of hardware to readout the pads and wires. For descriptions of the LabView programs used, see Section 3.3.

The DAQ hardware centers around CAMAC modules which acquire data and communicate with the computer. NIM electronics are used to distribute triggers to the CAMAC modules. Diagrams of the DAQ hardware systems are in Figures 3-1 and 3-3.

2.2.1 Charge distribution on pads

An analog pad signal must be converted to digital information by an Analog to Digital Converter (ADC) to be read out by the computer. To achieve the high density required, LeCroy 4300 and 4300B FERA[1] modules were used to readout the pads. Seven modules were available, each capable of sixteen channels of readout for a total capacity of 112 channels. Five FERAs were 9-bit, with a full-scale range of about 250 pC with a least significant bit (LSB) of 0.5 pC. Two were 11-bit, with a full-scale range of about 500 pC and a LSB of 0.25 pC. [11]

The 112 channel readout capacity is less than the number of pads, requiring that pads be selectively read out. With seven FERAs and 16 rows of pads, we opted to split each FERA across two pad rows and read out 8 pads from each of 14 rows. Cables 6 to 8 m in length, with 2×17 pin connectors at each end were used to connect

[1]FERA = Fast Encoding and Readout ADC

the TPC pad outputs to the FERAs. At the TPC end, the connectors were sawed in half in order to split each FERA between two rows. The wires leading from the ground pins on the FERAs were cut and soldered to connectors linking them to the ground pins on the TPC outputs, thus allowing the 8 channels per row to come from any location in each row.

The FERAs are charge integrating ADCs, meaning that they measure the total charge that arrives at an input over a period of time specified by a "gate" signal. The gate is delivered to the 4301 FERA Driver CAMAC module. The 4301, among other functions, takes a NIM level logic signal at its Gate input and distributes it via a ribbon cable to the 4300(B) FERAs.

2.2.2 Wire readout

The key feature of the wires in the TPC is to provide timing information for track reconstruction in the z-dimension. The discriminated wire signals are intended for this purpose. Using a 3 m ribbon cable with 2×17 pin connectors, half of the discriminated wire signals are brought to a logic signal level-converter in the NIM crate. Eight of these signals are then run to a LeCroy 2228A TDC. Unfortunately, this TDC (the best available) has a maximum range of 500 ns. This is not adequate for the several μs of drift time often associated with the TPC. The TDC, therefore, often returns no useful data. This is especially true when the trigger comes from the scintillators, as opposed to the wires.

To supplement the TDC information and keep a general record of wire pulse characteristics, the analog wire signals were also monitored. Using a LeCroy 9354A Digital Oscilloscope, four wire outputs were recorded during all data collection. The scope was set to trigger in External mode on a pulse provided by the main trigger system. The scope was read out by the computer over the same GPIB bus as the CAMAC crate.

Chapter 3

Measurements

Several sets of measurements were made with the TPC to confirm its functionality and evaluate its performance. An Americium-241 source from a smoke detector was used as a source of 5.5 MeV alpha particles. Cosmic rays were also detected using scintillators as a trigger.

3.1 Alpha source

The ^{241}Am source was mounted from the edge of the field cage, pointed parallel to the wire plane and perpendicular to the wires. It was mounted on the sixth field cage frame from the bottom, $6 \times 8\text{mm} = 48\text{mm}$ above the wire plane. This source emits 5.48 MeV alpha particles. [14] Using one of the sense wires as a trigger, tracks from individual alpha particles were collected. The pad readout region was arranged to be centered around the source.

3.1.1 Triggering

The alpha particles come randomly in time, so the only available trigger source is the TPC itself. The TPC signal wires were thus used as the alpha particle trigger. As shown in Figure 3-1, discriminated wire signals were made available at NIM logic levels via a LeCroy 4616 ECL-NIM converter. Then a wire could be selected to

provide triggers simply by plugging a Lemo cable into the desired output.

The selected wire logic signal was then passed into an AND gate (LeCroy 322G) also fed by a complementary output of the CAMAC pulse generator (LeCroy 4222 PDG). Quiescently, the latter signal is set to "True," and a signal from the TPC triggers the AND gate. This AND signal was then distributed to the oscilloscope trigger, the FERA gate, the 4222 trigger, and in later implementations, the TDC Start input. The trigger at the 4222 served to quickly (<200 ns) shift its complementary output to false, thus disabling the AND gate and blocking new triggers.

The FERA gate, controlled by a potentiometer on the 322G, was set to 500 ns. It was important to get this gate to the FERAs quickly after a wire signal, because the pad cabling was only 6 m (about 60 ns) long. At the end of a data cycle, the computer clears the 4222. This resets the complementary output and enables triggers from the wires to pass through the AND gate.

3.1.2 Measurements of Signal Shape as a function of Drift Field

The alpha source was also used for measurements of the TPC's wire signals as a function of drift field. With the sense wires kept at +2020 V, the drift voltage was varied from -500 V to -3700 V (for fields of 35 V/cm to 257 V/cm). While triggering on channel 4, pulses were recorded from channel 2.[1] This ensured that the measured pulses were from alpha particles that had not yet reached the end of their range, where dE/dx increases significantly. The data acquisition was performed exclusively by computer readout of the LeCroy oscilloscope, storing each waveform for later analysis.

Care was taken to avoid data contamination by factors other than electric field which can influence chamber performance. To ensure gas purity, the chamber was flushed before data collection and the flow rate was kept high (5-10 mL/sec) during measurements.

[1] See Figure 3-2 for an explanation of the wire channels.

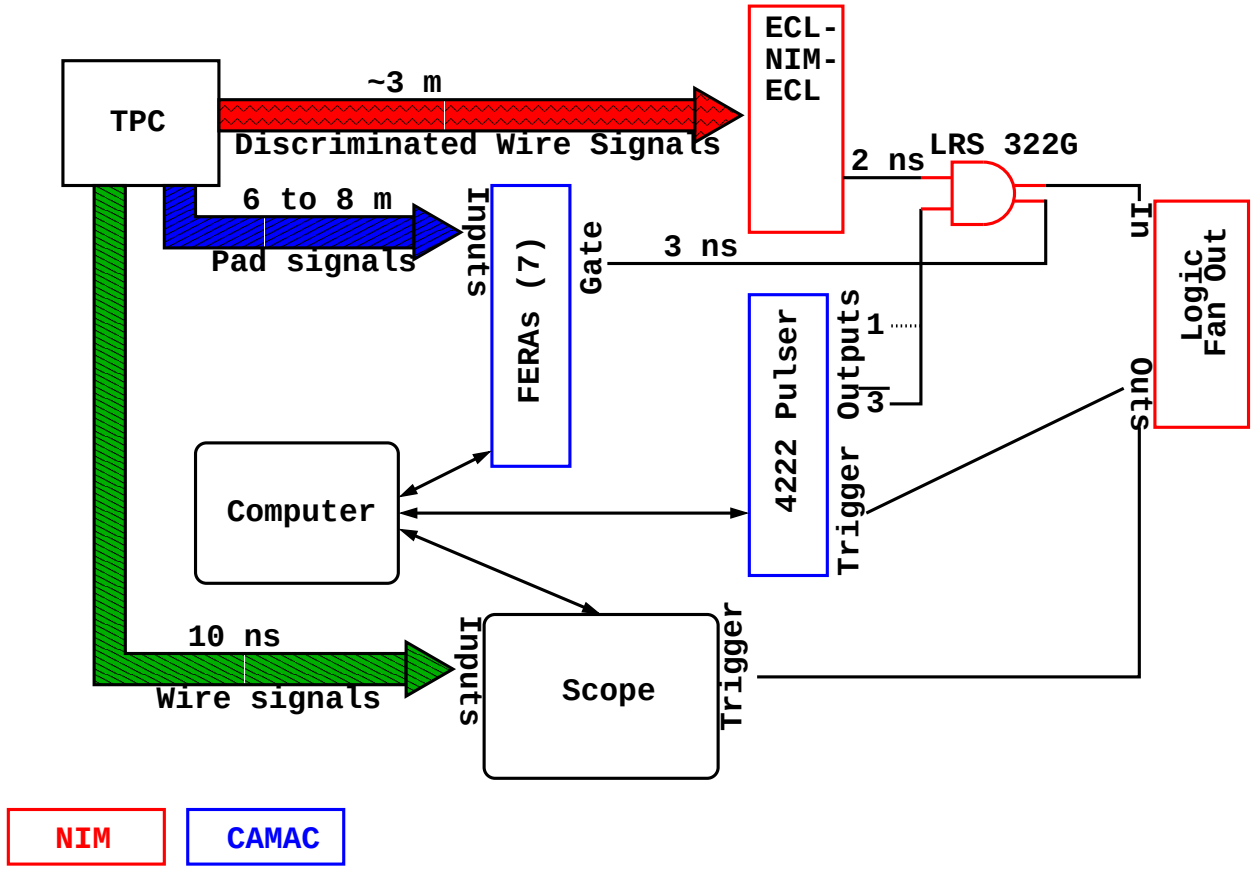

Figure 3-1: Electronics and connections for alpha particle readout using a sense wire trigger.

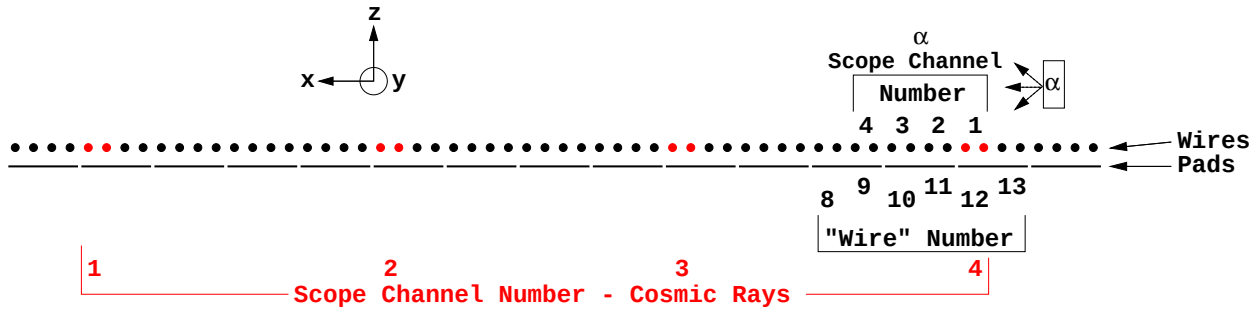

Figure 3-2: The x-z plane of the TPC, showing the ends of the sense wires. The identification numbers for wire pairs and the corresponding oscilloscope channels for alpha data collection are shown. The wire pairs used for cosmic ray events are shown in red. For cosmics, up is to the right.

3.2 Cosmic rays

A pair of scintillators was used to detect cosmic rays traversing the TPC. The cosmics gave tracks spanning the entire TPC length, allowing for testing of the entire pad readout area. For the cosmic data, the oscilloscope was connected to four wires spread evenly across the TPC, as shown in Figure 3-2.

3.2.1 Triggering

I wanted the detected cosmics to traverse the entirety of the TPC in the region where the pads were being read out. Therefore, the trigger was provided by a coincidence of appropriately aligned scintillators placed above and below the TPC. Unlike with a wire trigger, the scintillator signals appear at the moment the particle traverses the TPC. There is still a variable amount of time $t = \frac{z}{v_{drift}}$, as large as order μs but possibly small depending on the scintillator orientation, before the electrons drift to the wires.

The FERA gate, therefore, must arrive soon after the trigger and last several microseconds. This is best achieved with a pulse directly from the CAMAC 4222 pulser. A 2-fold coincidence of discriminated scintillator signals prompts a logic pulse to be distributed to the scope trigger, the 4222 trigger, and ADC gate (for the scintillators). The 4222, in turn, is programmed to generate a gate for the FERAs and (if necessary) a Start for the TDC. This electronics setup is diagrammed in Figure 3-3.

3.2.2 Scintillator Setup

For cosmic ray readout, the TPC was turned on its side so that the drift field was parallel to the floor (the gas exit was towards the ceiling). See Figures 3-7 and 3-6 for pictures of the TPC with scintillators. Because the readout region was a narrow strip of eight pads (48 mm wide), the scintillators were arranged to trigger only on cosmics that would leave complete tracks in the DAQ. Thus the bottom scintillator was oriented to allow a narrow width in y and a long range in z. The first trigger arrangement is shown in Figures 3-4 and 3-5. The top scintillator has dimensions

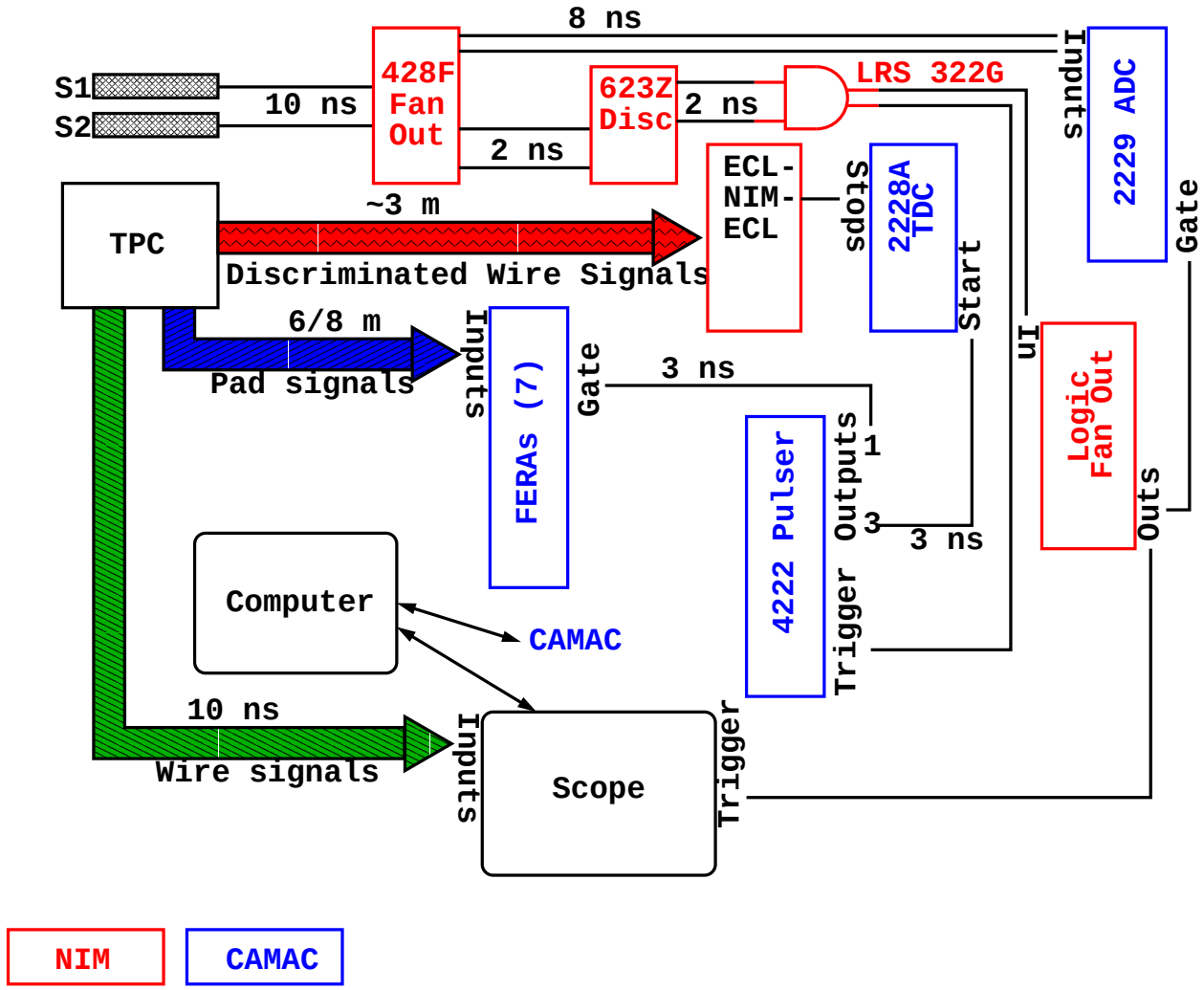

Figure 3-3: Electronics and connections for cosmic ray readout using a pair of scintillators (S1 and S2) as a trigger.

2×2×1 cm and the bottom scintillator 4.5×12×1 cm. For later data collection runs, the scintillators were moved to be centered with reference to the readout area.

The expected count rate R_μ for scintillator coincidences is

$$R_\mu = 2F_\mu \frac{A_{top}A_{bottom}}{2\pi d^2}, \tag{3.1}$$

where F_μ is the vertical cosmic ray muon flux, d is the scintillator separation, and A is the scintillator area. The value of F_μ at sea level is $\frac{1.08}{\text{cm}^2\text{min}}$. [17] Inserting the scintillator dimensions and a distance of 37 cm, $R_\mu = 3.8$ counts/hour. The observed rate was 4.0±0.4 counts/hour.

3.3 Recording procedure in TPC

The DAQ software on the PC was written using LabView 6. Separate software was needed for the alpha source data and the cosmic ray data, but many of the internal software components were modular and used in both programs. The software controlled many aspects of the data collection, including the configuration of the oscilloscope and collection of the data. Some controls, such as the high voltage settings, were set manually.

3.3.1 Calibrations and pedestal correction

In the first stage of software execution, data files are opened, the hardware is initialized, and calibrations are performed. First, the FERA modules are cleared and configured for the correct data readout mode. The other CAMAC modules and the oscilloscope are also initialized. If requested by the user, a calibration and pedestal correction are then performed. During data collection, these tasks were performed each time the CAMAC crate was power cycled.

The 4301 FERA Driver module is programmed by the computer with a digital value that corresponds to a voltage output. This voltage is transmitted to an input on the FERA modules, where it is applied to an internal capacitor. On a command

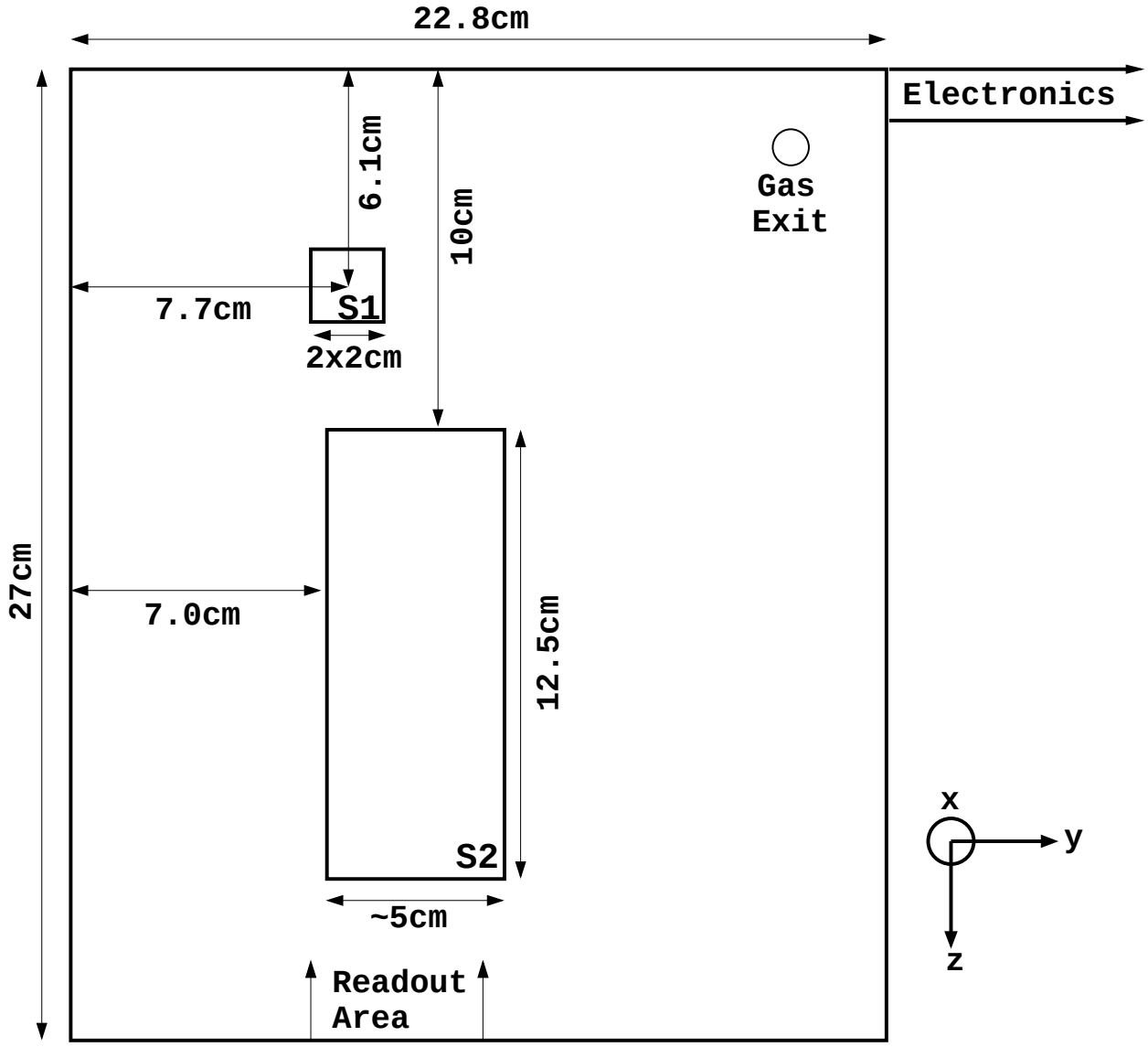

Figure 3-4: View of the y-z plane of the TPC, with projected scintillator positions.

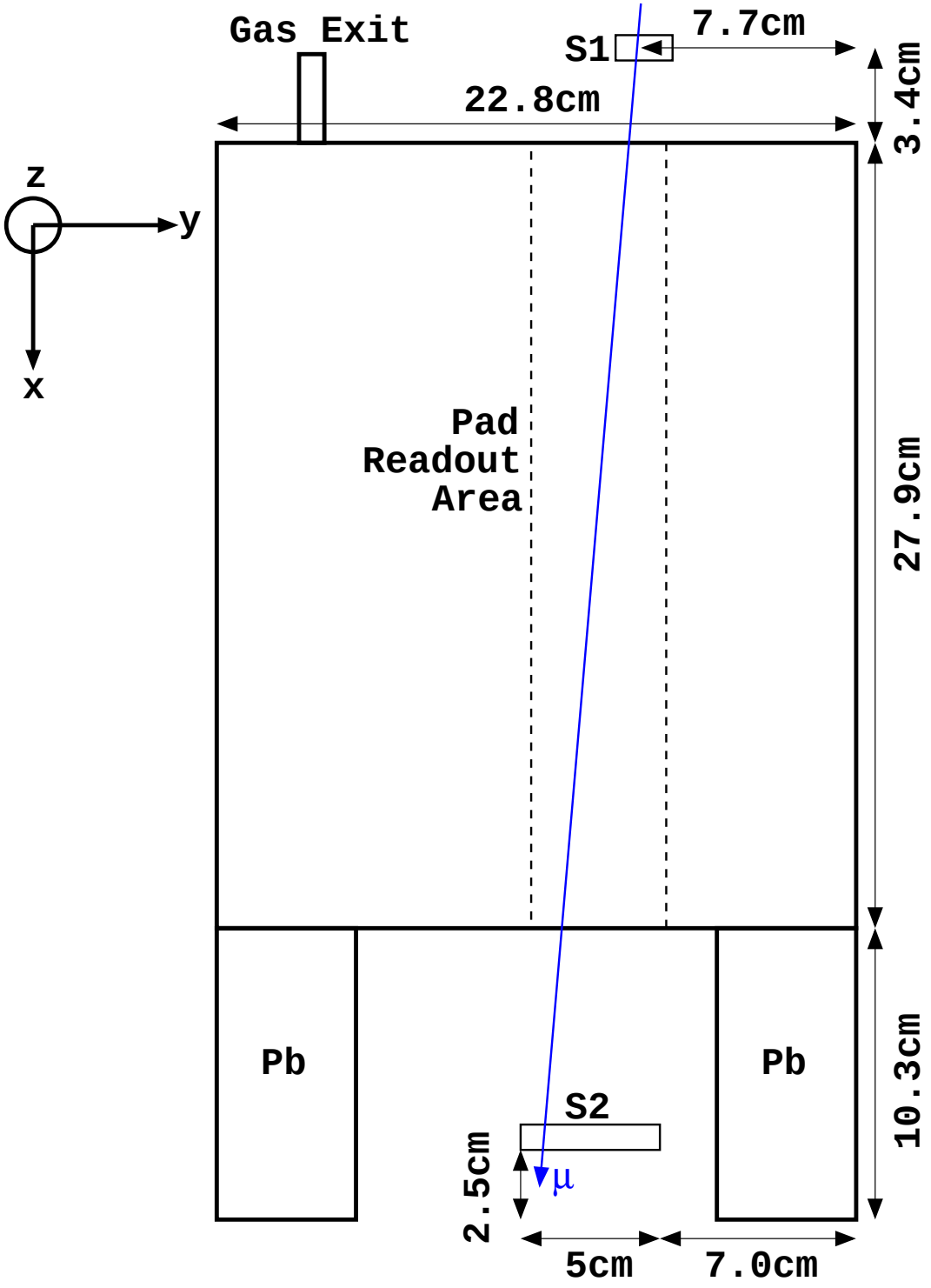

Figure 3-5: View of the x-y plane of the TPC, with initial scintillator positions. The blue line shows how a cosmic particle would travel through the TPC and both scintillators, creating a track to be read out on the pads.

from the computer, the FERA modules create a gate and apply this test charge to its analog inputs, just as if the charge had come from an external source. The resulting measurement of this charge, in the arbitrary units of the FERA scale, can then be read out by the computer as if it were normal data. My software used this feature to build a table with the FERA readings as a function of the test charge input for each FERA channel. After data collection, this calibration was used to convert the arbitrary FERA units into picocoulombs.

When a gate is applied, ADCs such as the FERAs inject a small amount of charge into each channel. [11] Any charge coming from the inputs themselves are measured on top of this "pedestal." The pedestal varies from channel to channel and with the width of the gate. To make proper measurements, the pedestal must be subtracted from the raw ADC readings. To facilitate this pedestal correction, my software generates artificial triggers which send gates to the FERAs.[2] The FERA readings from a number of these empty gates are averaged to determine the pedestal for each FERA channel. During this procedure, the input cables are left connected as normal (for proper termination of the inputs), but the power to the amplifier is switched off to ensure that no signals from the TPC come to the FERAs. Once the pedestals are measured, they are programmed into the FERAs and an option is enabled which automatically subtracts them from the FERA data.

3.3.2 Data readout

The data collection section of the software is a large loop where the program spends most of its time. The first step is a subloop which repeatedly checks the LAM status of the FERAs.[3] During initialization, the FERAs are configured to generate a LAM whenever they receive a gate.

[2]The exact method employed to produce these gates depends on the type of trigger. In both cases the gate to the FERAs for the pedestal correction is exactly the same gate used for actual data collection.

[3]LAM, or Look at Me, is a standard CAMAC status signal for determining when a module has data.

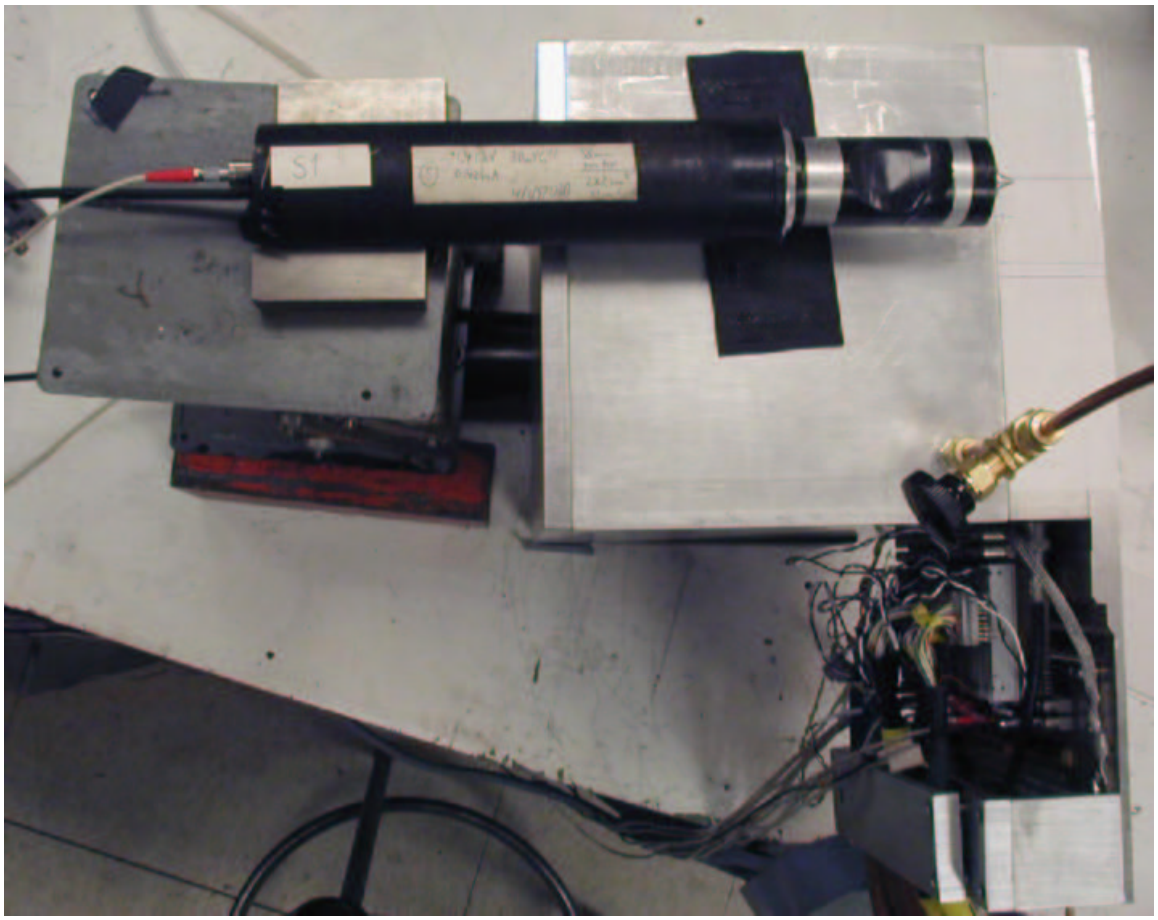

Figure 3-6: View of the y-z plane of the TPC, showing the top scintillator (S1) in its initial position.

When all of the FERAs report a LAM signal, data readout proceeds.[4] To disable any additional data input, the Inhibit status of the CAMAC crate is turned on. The FERA modules are read out sequentially, the oscilloscope data is acquired, and additional CAMAC data modules (*e.g.* a TDC and ADC) are read out. The data from these sources are displayed on screen and written to the open data files. To complete a data cycle, the data registers on the various modules are cleared and the 4222 PDG is reset. Finally, the Inhibit signal is cleared. The system is then ready for another trigger, and the program returns to the beginning of the data readout loop.

[4]LAM is returned for all gates, whether or not any charge is detected.

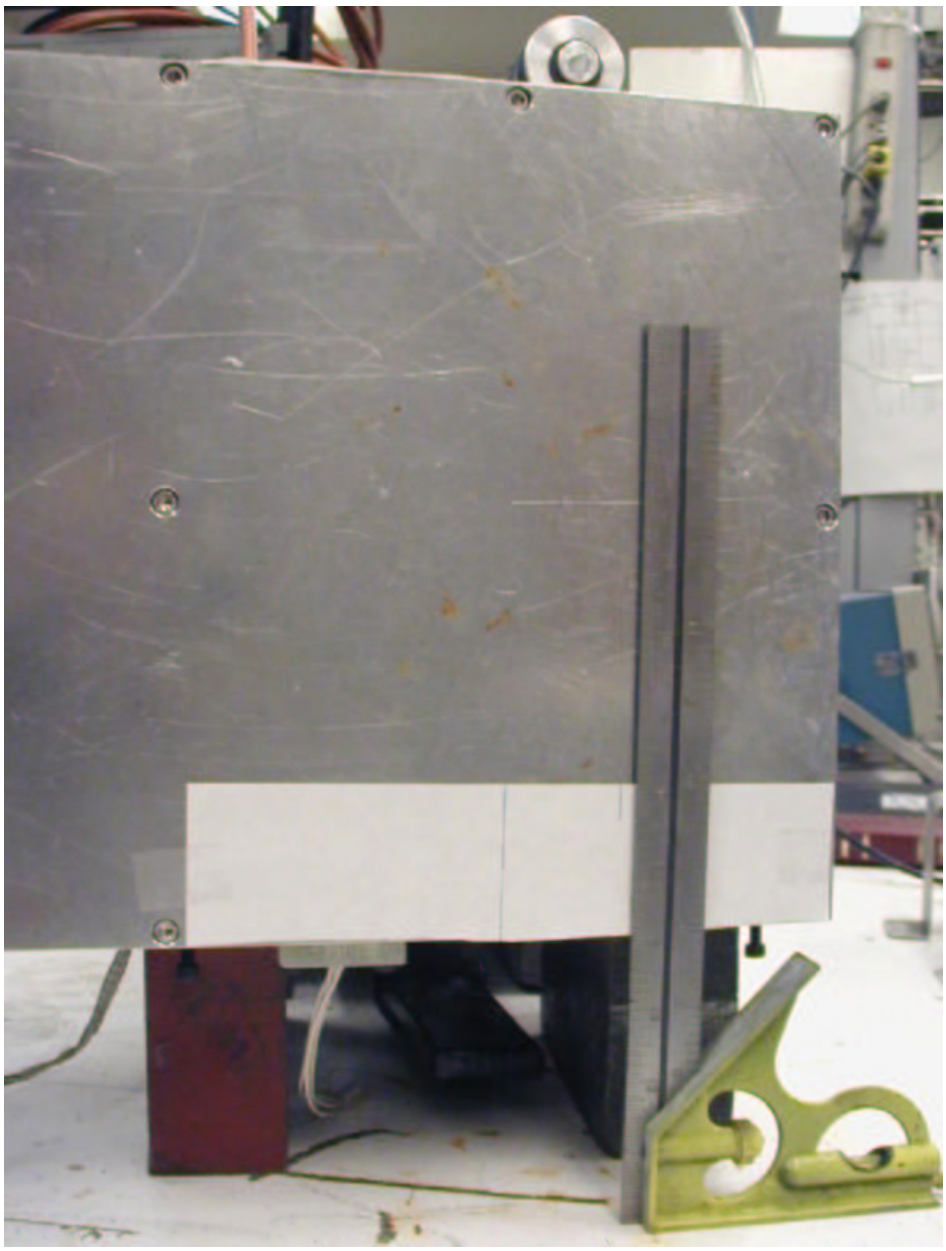

Figure 3-7: View of the x-y plane of the TPC, with initial scintillator positions.

Chapter 4

Data and analysis

4.1 Alpha particles

Alpha particle event rates were high, as shown in Figure 4-1. Over 500 alpha particle events were collected for the range analysis in section 4.1.1. A sample alpha particle event, with pad and oscilloscope data, is shown in Figures 4-2 and 4-3.

From Figure 4-2, several features of this event can be determined. First, because the signals on channels closer to the source come after the signals from further channels, the alpha particle had a downward (towards the wire plane) trajectory. The size and timing of the signals on Channels 3 and 4 give an indication as to the range projection in the x direction. The small signal size on Channel 4 combined with the small time difference (14 ns, when measured using the 10% levels of the peaks) compared to the other channels means that the alpha did not quite reach the wires corresponding to Channel 4. The charge seen on Channel 4 diffused from the end of the particle track over or just past the Channel 3 wires.

The alpha source location was measured with a ruler to within a few millimeters of the location shown in Figure 4-3. The location shown was determined using best fit pad trajectories such as the one indicated by the green line. Superimposing a number of these best fit tracks gives the best estimate of the source location, as shown in Figure 4-4.

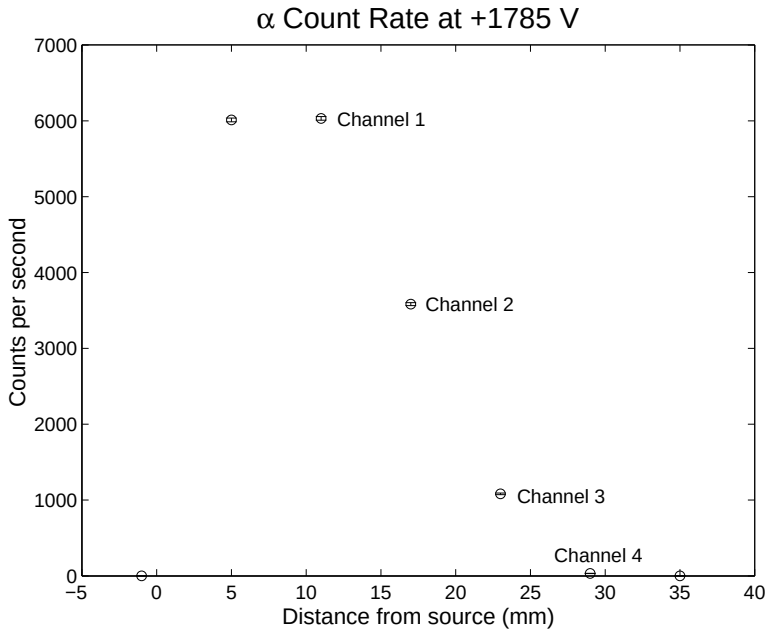

Figure 4-1: Event rates as measured by a scaler connected to the TPC's discriminated wire outputs. The Channel labels refer to oscilloscope channels receiving signals from a wire doublet.

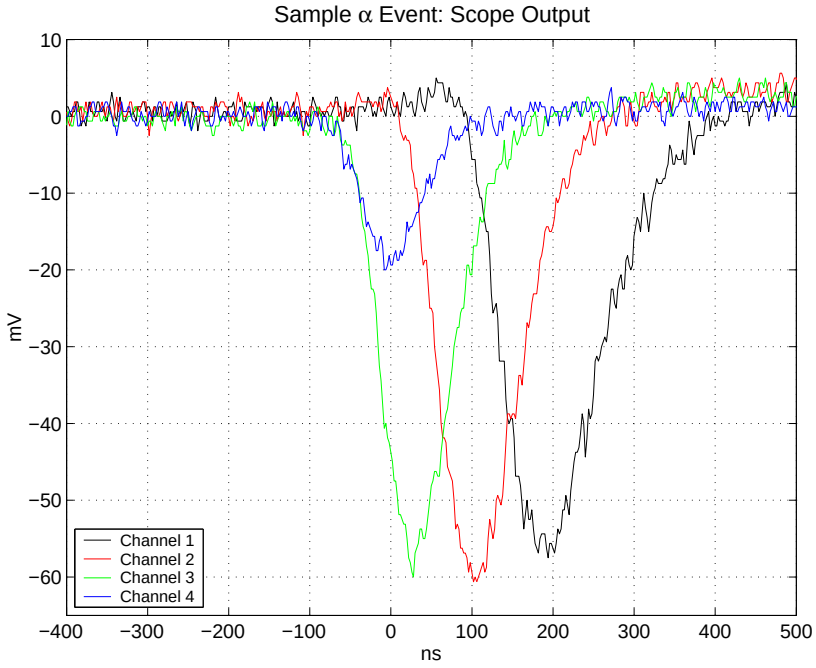

Figure 4-2: Oscilloscope output of a sample alpha particle event. The trigger for this event came from the wire on oscilloscope channel 4.

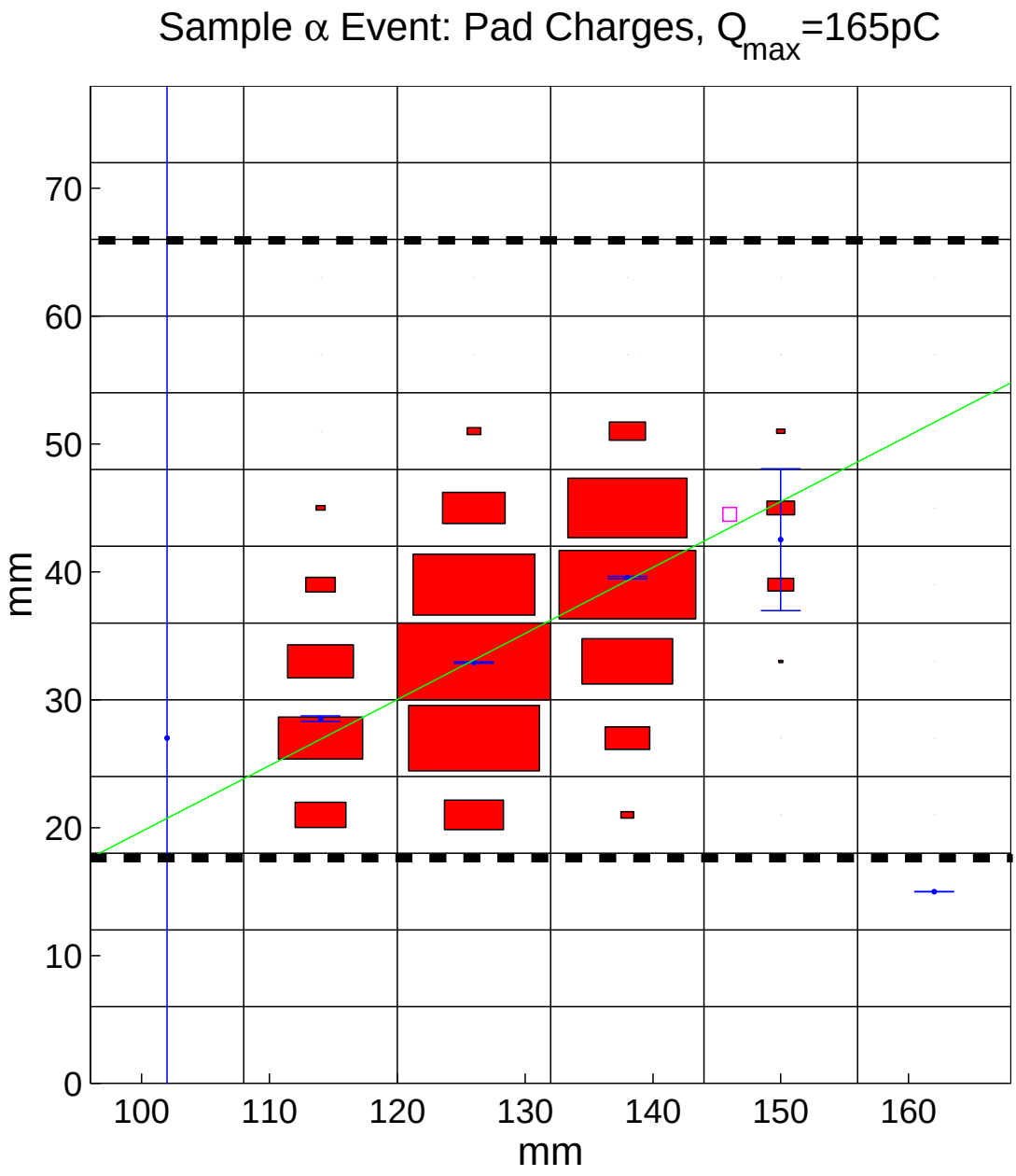

Figure 4-3: Pad output of the sample alpha particle event shown in Fig. 4-2. The area of each filled rectangle is proportional to the charge on the pad, normalized to the maximum charge Q_{max}. The points are the centers of charge calculated using eq. 4.6, with the best fit line shown in green. The purple square is the location of the alpha source, and the dashed lines outline the active readout area. For a description of the fitting procedure, see Section 4.2.1.

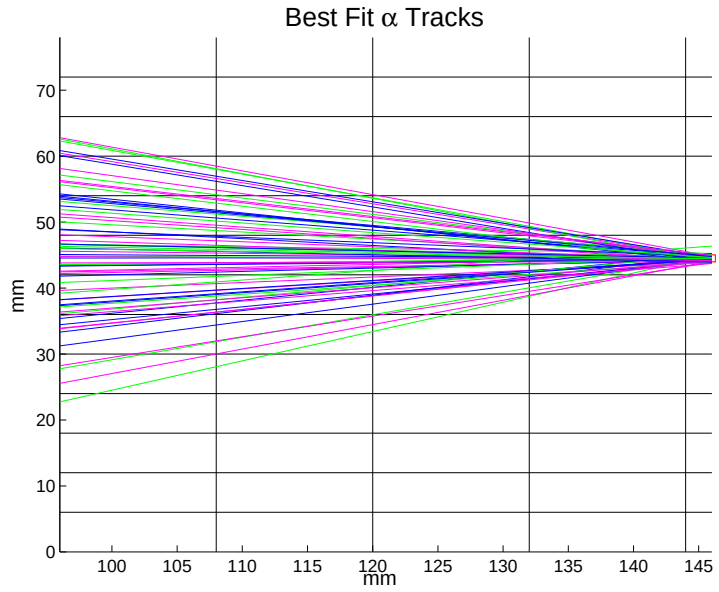

Figure 4-4: The crossing point is the location of the alpha source, as determined by the crossing point of these tracks. The colors of the tracks represent the trigger wire. Green=Wire 8, Blue=Wire 9, Magenta=Wire 10

4.1.1 Range determination

A heavy charged particle such as an alpha particle loses energy at a rate whose mean is given by the Bethe-Bloch equation,

$$-\frac{dE}{dx} = K\frac{Z}{A}\frac{z^2}{\beta^2}\left(\ln\frac{2m_e c^2\beta^2\gamma^2 W_{max}}{I^2} - 2\beta^2 - \delta\right), \tag{4.1}$$

where $K = 2\pi N_A r_e^2 m_e c^2$. Here N_A is Avagadro's constant, r_e is the classical electron radius, m_e is the electron mass, z is the charge of the incident particle, Z and A are the atomic number and mass of the medium, and β is the particle velocity in units of c. W_{max} is the maximum kinetic energy which can be given to a free electron in a collision with the incident particle (the energy transfer from a kinematic head-on collision), I is the mean excitation potential of the medium, and δ is a density effect correction. dx is measured in mass thickness units of g/cm^2. [12]

By integrating up to the initial particle energy T_0, Equation 4.1 can be applied to determine an ionizing particle's range R,

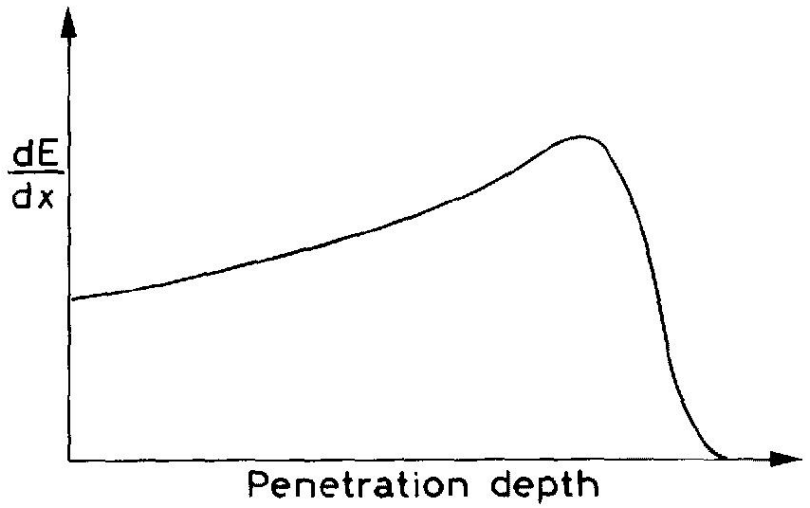

Figure 4-5: The general form of dE/dx as a function of distance from the particle source. [12]

$$R = \int_0^{T_0} \frac{1}{dE/dx} dE. \tag{4.2}$$

However, the Bethe-Bloch equation is not valid for very low energies, so in practice the integral in equation 4.2 cannot be taken from a lower bound of zero. Empirical data must be used. Figure 4-5 shows a plot of dE/dx as a function of distance from the particle source. Bethe-Bloch behavior is demonstrated to the left of the dE/dx peak, with ionization increasing with decreasing β^2. The violation of this model can be seen at the end of the range, where dE/dx drops rapidly. [12]

The empirical ranges of alpha particles in various media are well known. A calculation using equation 4.2 combined with empirical data for energies < 2 MeV yields ranges of 7.508×10^{-3} g/cm^2 and 3.142×10^{-3} g/cm^2 in argon and CH_4, respectively. [8] Dividing by the appropriate densities and weighting for the gas fractions, the range in P10 is found to be

$$R_{\mathrm{P10}} = (0.9) \quad \times \quad \frac{7.508 \times 10^{-3}\mathrm{g/cm}^2}{\rho_{\mathrm{Ar}} = 1.784 \times 10^{-3}\ \mathrm{g/cm}^3} +$$

$$(0.1) \quad \times \quad \frac{3.142 \times 10^{-3} \text{ g/cm}^2}{\rho_{CH_4} = 0.893 \times 10^{-3} \text{ g/cm}^3} = 4.14 \text{ cm}. \tag{4.3}$$

The alpha particle range for each event was found using a software script. The range in the x direction (perpendicular to the wires and parallel to the wire plane), was primarily determined from oscilloscope data. The deflection in the y direction (the angle parallel to the wire/pad plane) was calculated from a best fit of pad data. The z direction (the angle with the wire/pad plane) was found using the timing of wire signals. The total range is then given by $\sqrt{x^2 + y^2 + z^2}$.

Histograms of the measured range are shown in Figure 4-6. Some alpha particles did achieve a range between 4 and 5 cm, comparable to the expected value of 4.1 cm. The vast majority of alphas, recorded while triggering on wires closer to the source, had ranges <4 cm. This is attributable to the source. The ^{241}Am is of finite thickness, and the source is coated for safety reasons. Most of the alpha particles lost some of their energy, either in the coating or the source material itself, before entering the detector volume.

Effects of reduced pressure

As calculated in equation 4.3, the expected range of an alpha particle in a material is inversely related to the material's density. Therefore, an effort was made to operate the TPC at reduced pressure in order to see longer tracks. Pad data was collected for several events at a chamber pressure of 420 Torr. Figure 4-7 shows a particle track that was leaving the instrumented region of the pads. The oscilloscope output for that event is shown in Figure 4-8.

Compare this event to that of Figure 4-3. The particles left the alpha source at similar angles in the x-y plane, but the event at lower pressure ionized less densely and had a longer range.

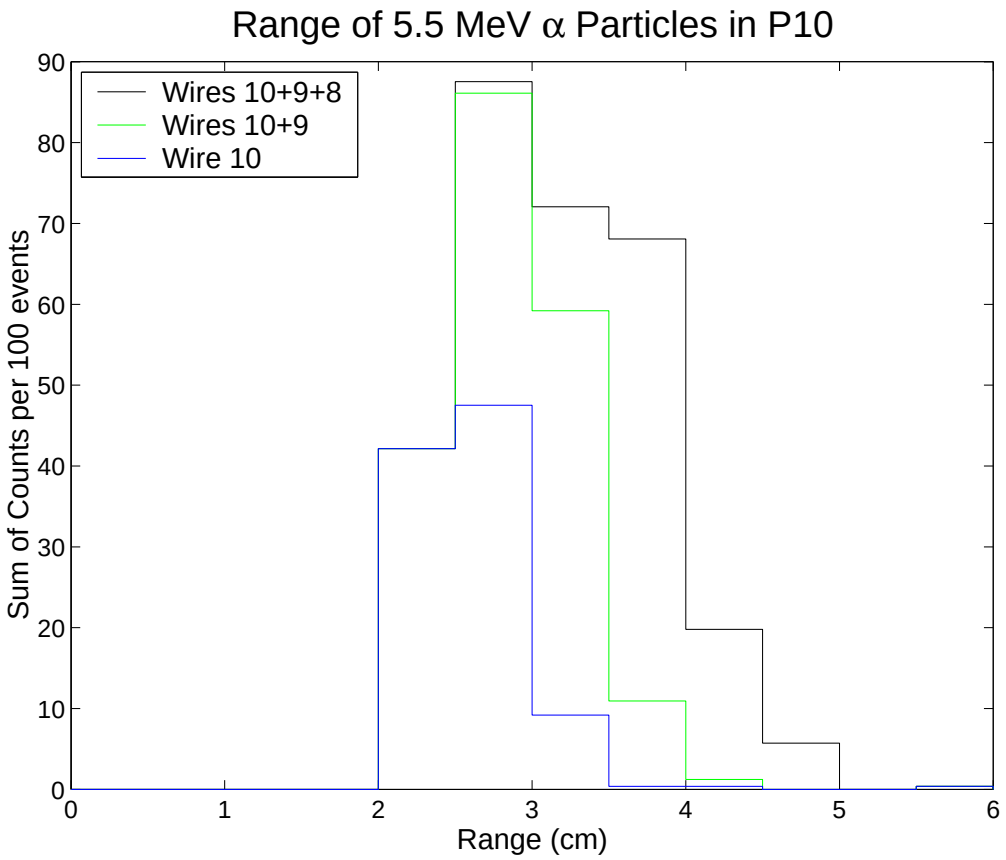

Figure 4-6: Range data collected using several different wires as trigger. For a key to the wire numbers, see Fig. 3-2. For each wire, the number of counts in each bin is normalized to the total number of counts in the data set. The data sets are then summed as indicated by the legend.

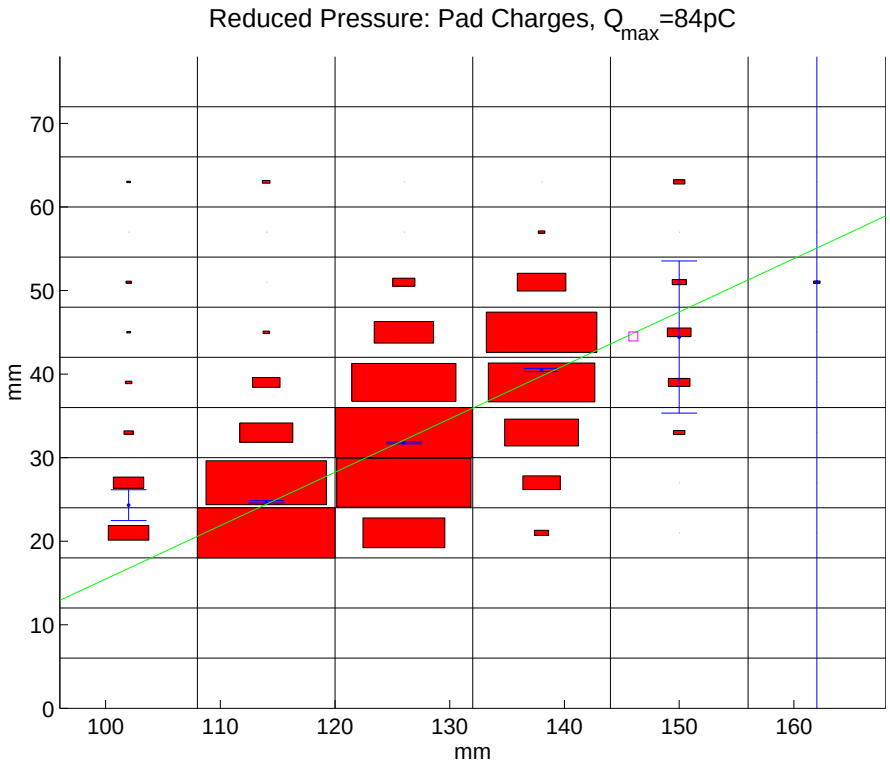

Figure 4-7: An event taken at 420 Torr. Note that the particle traveled in a path long enough that its charge distribution is cut off at the edge of the detected region of the pads. (The bottom three pads of each row were not being read out.)

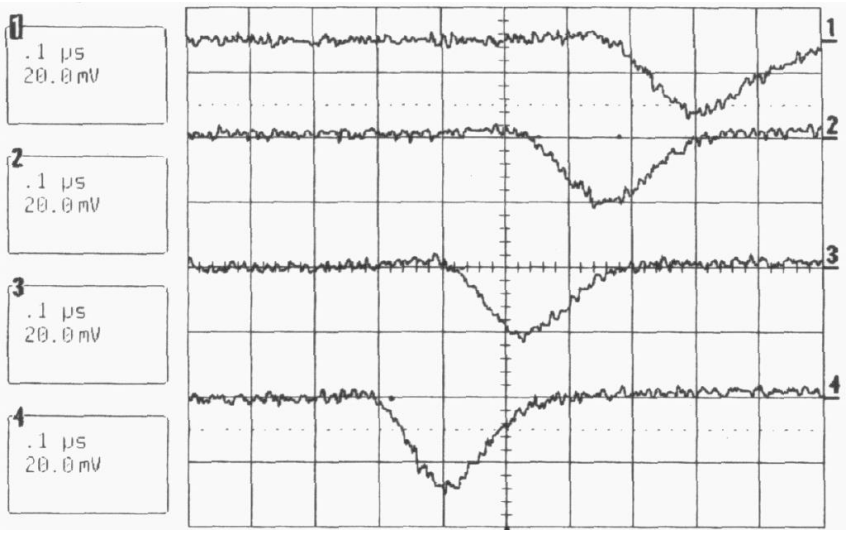

Figure 4-8: Reduced pressure: Oscilloscope data to accompany Figure 4-7. Scale: 0.1 μs/div, 20 mV/div

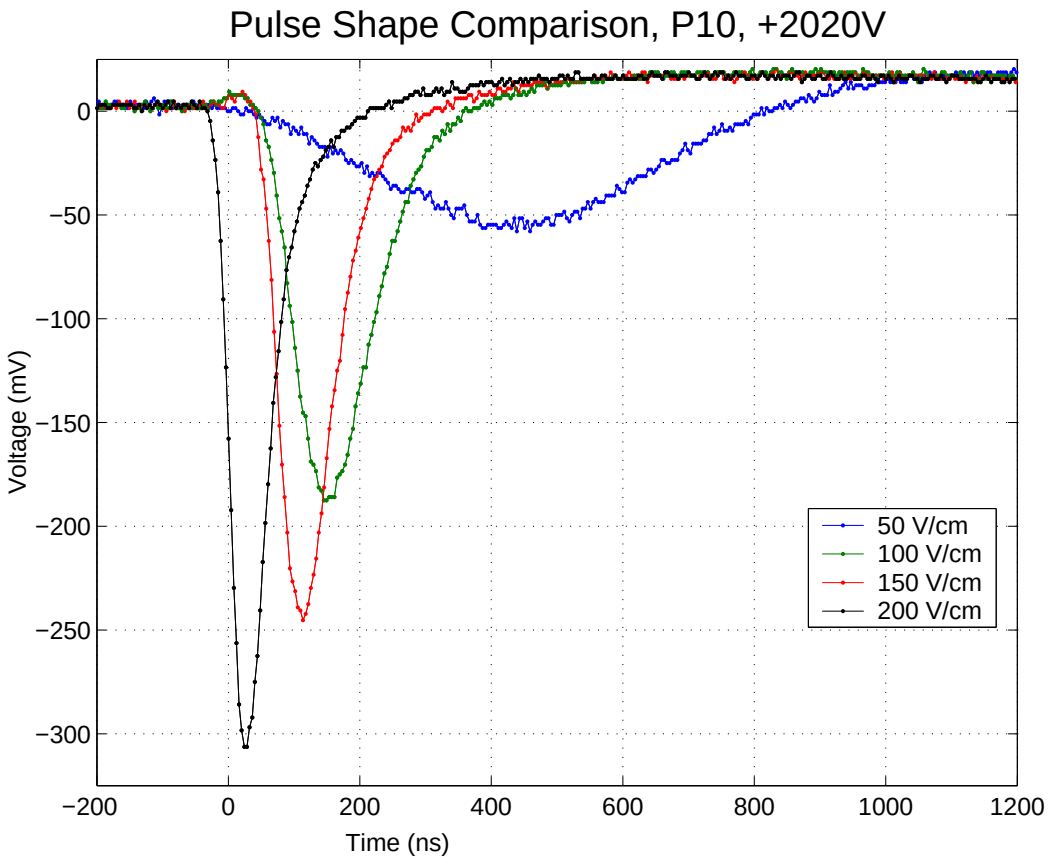

Figure 4-9: Alpha particle wire pulses at varying drift fields.

4.1.2 Measurements as a function of drift field

The waveforms of wire signals from alpha particles were collected as a function of drift field. Example pulses taken at several fields are shown in Figure 4-9. Approximately 400 samples were taken per field setting.

Calculation of total charge

Electrons drifting in a chamber may be attenuated for several reasons. They can recombine with positive gas ions. Also, certain gases with a high electronegativity can dramatically affect chamber performance through attachment, the process by which a drifting electron attaches to a neutral atom to form a negative ion. Due to the strong attachment properties of oxygen, air contamination can lead to a rapid

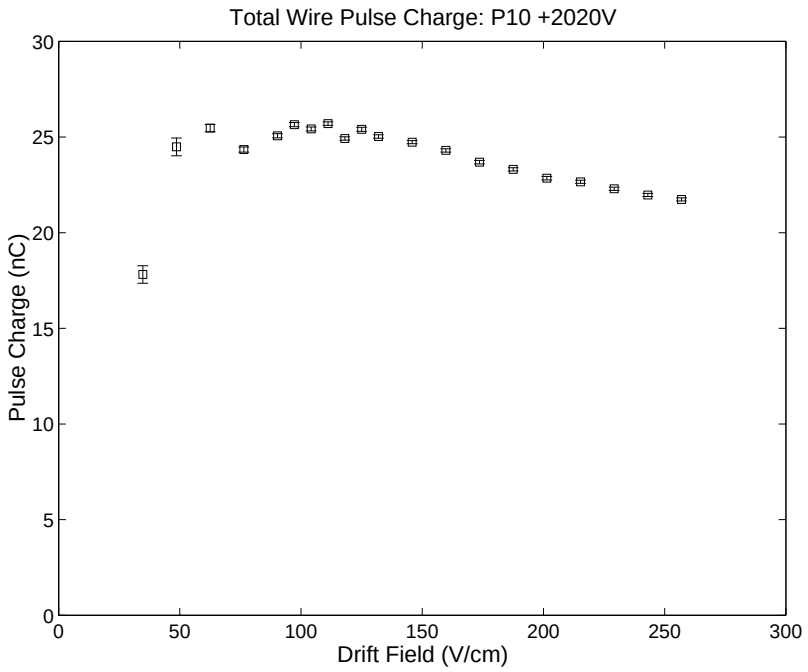

Figure 4-10: Average integrated wire charge generated by the alpha source.

decline in chamber performance. [12]

Attachment becomes more severe as drift times increase, because the intrinsic electron velocity is high compared to the drift velocity and governs the number of collisions. Therefore, a reduction in electric field, and thus drift velocity, could lead to increased attachment and decreased performance.

A Gaussian curve was fit to each data waveform. These Gaussians were then integrated numerically to determine the total charge present. No attenuation of the wire signals was observed until very low fields, about 50 V/cm, as is shown in Figure 4-10.

Calculation of risetime as a measure of longitudinal diffusion

Ionization electrons diffuse with time, acquiring a Gaussian distribution

$$\frac{dN}{dx} = \frac{N_0}{\sqrt{4\pi Dt}} \exp\left(\frac{-x^2}{4Dt}\right), [12] \tag{4.4}$$

where N_0 is the normalization, x is the distance from the initial point of ionization, and D is the diffusion coefficient. The rms spread in x is thus $\sigma_x = \sqrt{2Dt}$. For a drift velocity v, this becomes

$$\sigma_x = \sqrt{\frac{2D}{v}}\sqrt{d}$$
$$\frac{\sigma_x}{\sqrt{d}} = \sqrt{\frac{2D}{v}}, \tag{4.5}$$

when the electrons drift a distance d.

The output signal from the wires is the integrated deposited charge. Therefore, for each sample, dS/dt was calculated point by point for the rising edge of the signal. This gave a curve in the Gaussian form of equation 4.4 with a width σ_t. The diffusion as expressed in equation 4.5 is then found using $\sigma_x = \sigma_t v$. The mean drift distance d was taken to be the height of the alpha source, 4.8 cm. A theoretical calculation of the diffusion was made using the Magboltz program. Magboltz generates the diffusion coefficient D and the drift velocity v, allowing calculation of the diffusion $\sigma_x/\sqrt{d}$. [4]

4.2 3-D tracks of cosmic rays

The pattern used for the readout of the TPC pads was optimized for long tracks in a narrow angular range. The alpha particles did not provide tracks nearly long enough to test the entire length of the TPC. Cosmic rays were a natural substitute.

Extending the Bethe-Bloch equation (4.1) to high energies, dE/dx drops as energy rises until it reaches a minimum at about $\beta = 0.96$. For still higher energies, ionization increases slowly. The peak of the cosmic ray muon energy spectrum sits near the minimum ionizing point. [17] This fact combined with the small charge of the muon compared to an alpha particle implies that cosmic rays ionize much less heavily than the alpha particles.

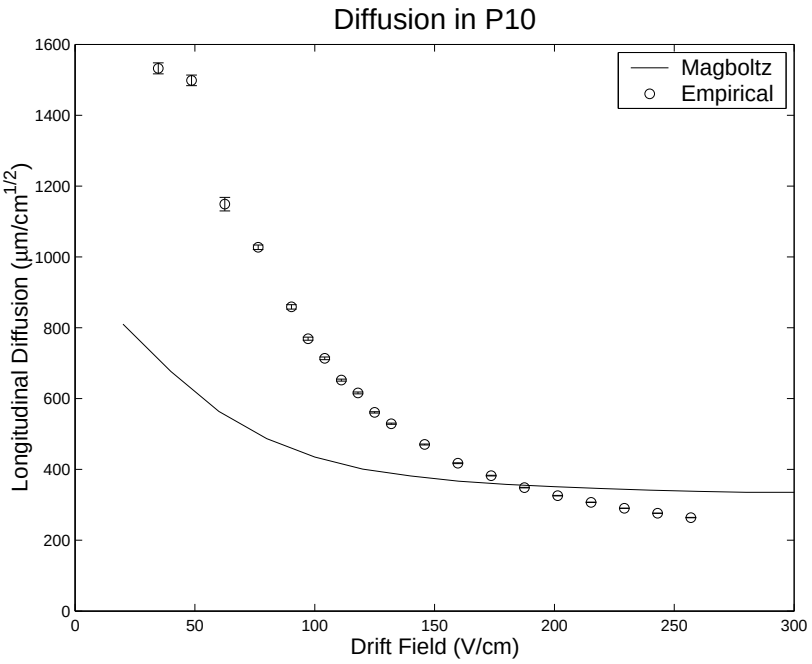

Figure 4-11: Diffusion in Argon:CH_4 (90:10)% as a function of drift field. Points are derived from the derivative of the rising side of alpha event wire signals and the curve is generated by Magboltz.

4.2.1 x, y reconstruction with pads

The pad readout and plotting shown for alpha particles in Figures 4-3 and 4-7 were put to their fullest use in the analysis of cosmic tracks. Figure 4-12 shows a sample cosmic track. The wire voltage was set to +2350 V, and the drift field was 154 V/cm (−2225 V). Despite the relatively high voltage, the ionization due to the muons was low compared to the slow alphas.

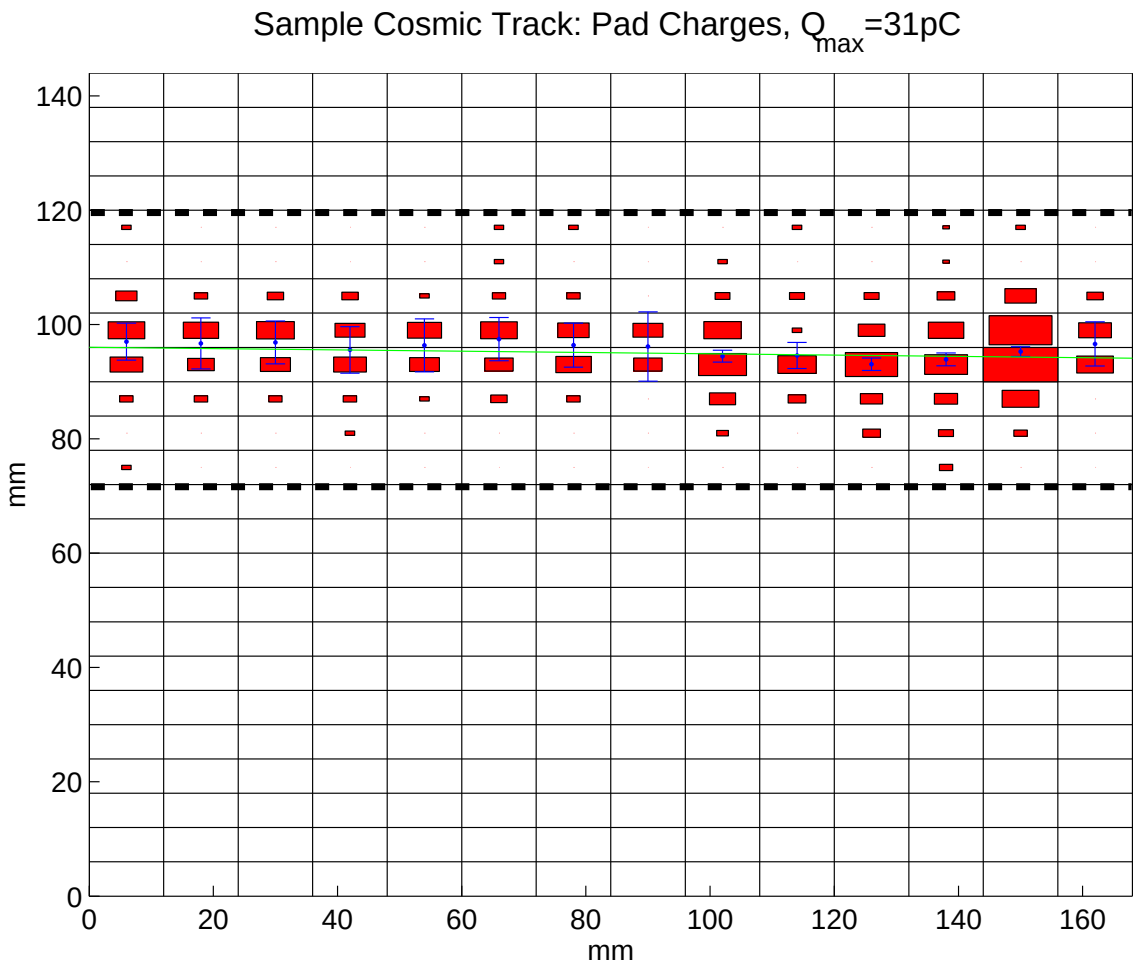

Figure 4-12: Track of a cosmic ray. The dashed lines outline the active readout area. The direction of the ceiling is to the right on the graph.

To determine the best fit (green) track, each pad row is taken separately, where a row is oriented perpendicular to the particle path. For each row of 8 pads, the center

of charge y_q is determined by the center of gravity method,

$$y_q = \left(\sum_i^8 y_i q_i \right) / \left(\sum_i^8 q_i \right), \tag{4.6}$$

where y_i and q_i are the center and charge of the ith pad. When using this method, care must be taken that pedestals are subtracted properly and that the full width of the ionization be measured for each pad row. Otherwise, y_q will be biased towards the center of the readout area.

The error for each pad measurement is taken to be ± 1 ADC Unit. This error is propagated through equation 4.6 to generate the error bars shown in Figure 4-12. A least squares fit is performed on all rows with non-zero total charge. Because the error bars are taken into account by the fit, rows with only a small amount of charge (*e.g.* in the alpha data, a row with only noise and no real charge) and a large error bar have appropriately minimal influence on the fit.

4.2.2 z reconstruction with wires

Despite the lack of TDC data to determine wire timing, some of the cosmic tracks do have several channels of oscilloscope data. The pulses shown in Figure 4-13 are an excellent example. The raw data from the scope and a plot of the timing of these pulses versus x distance are shown. The best fit line on the second plot allows for reconstruction of the x-z track by $z = v_{drift}t$. By hand, I selected 18 events with 4 identifiable wire signals. These events were fed into a computer script which found the 10% level of each peak and produced the fit track.

4.2.3 Track resolution

Cosmic ray events were used to measure the resolution in both the x-y and x-z planes. For each data point, the difference between the measured value and the value from the fit track was taken. The width σ of a histogram of these residuals gives the resolution. Diffusion, the inherent detector resolution, and the track angle all contribute to the

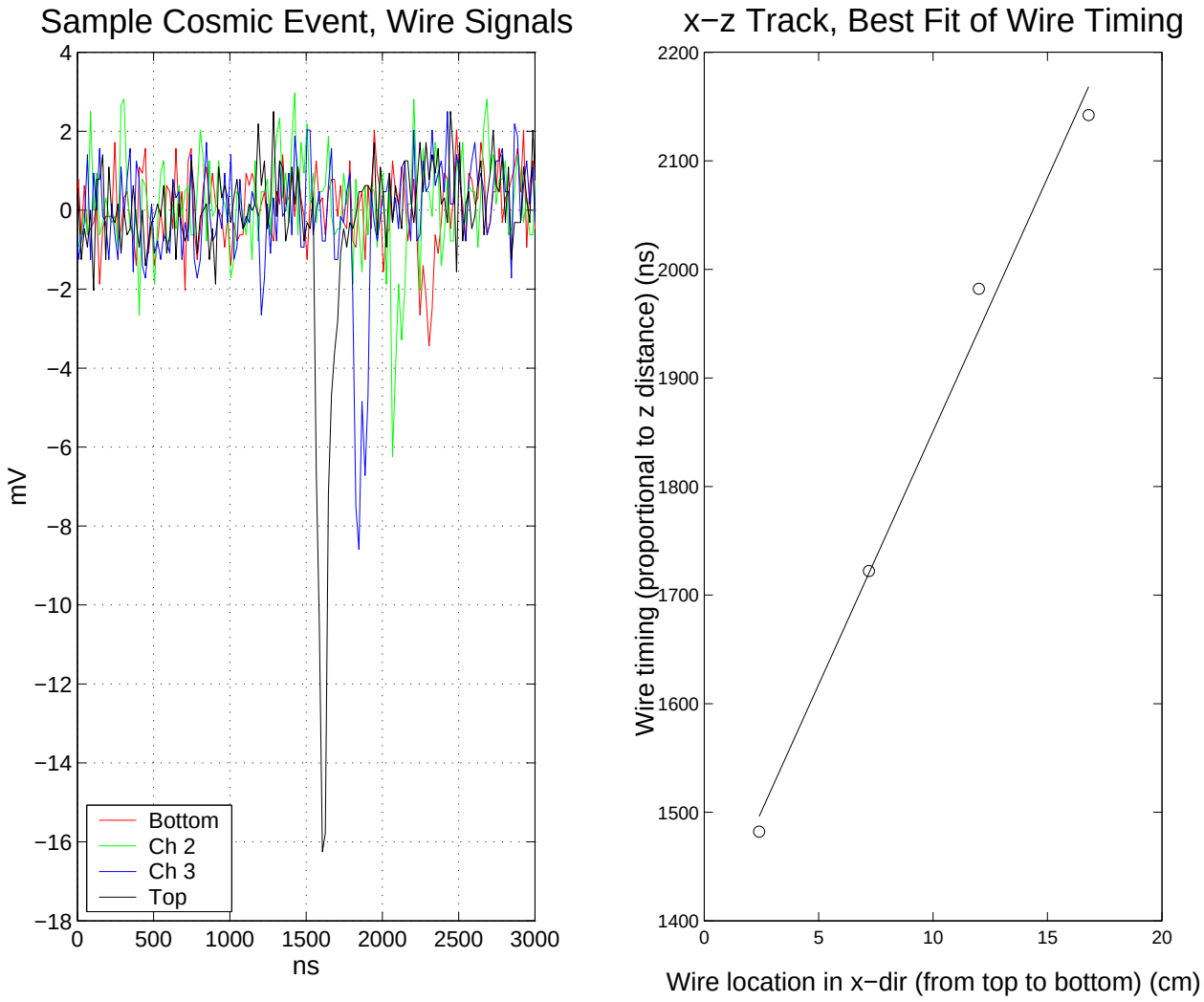

Figure 4-13: Wire signals to accompany the track shown in Figure 4-12. The scope channels were connected to evenly spaced wires along the TPC (see Figure 3-2). The plot on the right shows the best fit of these signals. The measured time corresponds to the drift distance in the z direction.

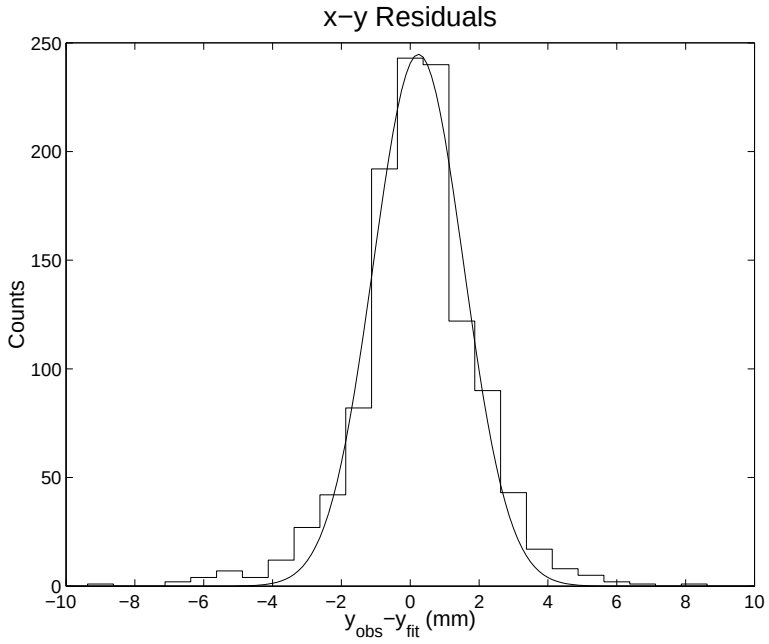

Figure 4-14: Residuals from pad data. Aggregate data from 82 cosmic ray events. Gaussian fit parameters: $\sigma = 1.3$ mm, mean $= 0.24$ mm

measured σ. [6, 9]

For pad data, only tracks which were completely contained inside the readout area with no edge effects were used for residuals analysis. For wire data, only tracks in which all 4 scope channels had signals were used. A histogram of the x-y plane residuals, derived from pad data, is shown in Figure 4-14. x-z residuals, from wire timing data, are shown in Figure 4-15.

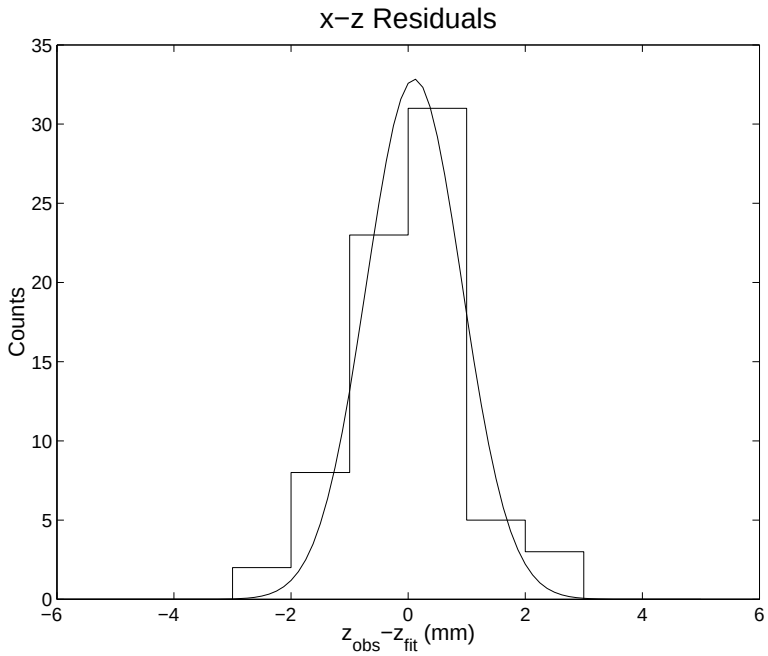

Figure 4-15: Residuals from wire data. Aggregate data from 18 cosmic ray events. Gaussian fit parameters: $\sigma = 0.8$ mm, mean $= 0.10$ mm

Chapter 5

Summary

A TPC was set up and connected to a CAMAC crate for readout. Using a 5.5 MeV alpha source, the sense wire pulse risetime and charge were measured as a function of drift field. These measurements were used to estimate the longitudinal diffusion in P10 and verify that charge was not being significantly attenuated over the drift distance. Alpha particle tracks were reconstructed from wire and pad data. The predicted range of 4.1 cm was confirmed, although considerable straggling was observed, probably due to the thickness of the source.

The complete pad readout area was tested using cosmic rays as triggered by a pair of scintillators. Residuals for tracks in the x-y and x-z planes, reconstructed using pad charges and wire timing respectively, were collected. The lateral (x-y) resolution was found to be 1.3 mm. The longitudinal (x-z) resolution was found to be 0.8 mm.

The Gas R&D group at MIT has been working with GEMs for several years. [18] In the future, GEMs will be added to the TPC in order to eliminate the signal wires. This research with pads will be immediately applicable. The detector proposal for the planned TESLA experiment calls for a TPC using either GEMs or other novel technologies. [3]

Appendix A

Data collection instructions

An overall note: The programs will at various times before data collection ask for confirmation to replace various files. The user should click "Replace" to confirm the replacement of these files.

A.1 Wire-Based Trigger

The following are step-by-step instructions for the collection of alpha particle events.

Setup

1. Power on NIM and CAMAC crates
2. Power on scope (Trigger should be External)
3. Do not power on ± 5 V or HV
4. Start gas flowing
5. On NIM crate, one Lemo cable is plugged into the ECL-NIM-ECL module. The position of this cable determines the trigger wire. A key to the the wire numbers is found in Figure 3-2.
6. Set switch on 322G Logic unit (NIM) to "OR" position.

7. If not already loaded, load the `alpha_readout_continuous_tdc.vi` program in LabView.

Procedure

8. Make sure the button "Take Scope Data" is illuminated.

9. If you wish to collect data points one at a time, place the switch in the middle of the screen in the "User Iterate" position. If you wish to have data continuously collected, place the switch in the "Continuous" position.

10. If the CAMAC power has been cycled since the last calibration, turn on the switch labelled "Take New Calibration?" If no new calibration is needed, then turn this switch off.

11. Run the program by clicking the white arrow in the upper left hand corner.

12. A box pops up asking for a file name. This will be the name of the pad data file. The name must end in ".log".

13. A calibration is performed which takes about 5 minutes. This stage is over when the program asks you to confirm replacement of "trv_all.log".

14. Pedestals are measured, ending with the program asking to replace "pedestal.log".

15. Move the switch on the 322G to "AND."

16. Turn on the HV and ± 5 V.

17. If you are in "User Iterate" mode, data is collected by clicking the "Iterate" button at the center of the screen. If you are in "Continuous" mode, data is already being taken.

18. To stop taking data, click "Cancel."

A.2 Scintillator-Based Trigger

The instructions that follow are a guide for collecting data with the scintillator/TPC system.

1. Turn on power to the CAMAC and NIM crates. Turn on power to the oscilloscope.

2. Start gas flow.

3. If not already loaded, load the `cosmics_readout_tdc.vi` program in LabView.

   (a) If the CAMAC power has been cycled since the last calibration, turn on the switch labelled "Take New Calibration?" If no new calibration is needed, then turn this switch off.

   (b) Make sure the CAMAC slots are set correctly (they should be).

   (c) Adjust the Gate and Delay settings if necessary. The default of a 4000 ns gate after a delay of 200 ns is probably correct.

   (d) Run the program by clicking the white arrow in the upper left hand corner.

4. You will be prompted for the datafile name. Enter a name in the dialog box.[1]

5. As instructed by the computer program, disconnect the two analog inputs to the 2229 ADC. Replace them with 50Ω terminators.

6. Set the switch on the 322G logic unit to the OR position.[2]

7. Hit the "Done" button on the computer. The computer then takes a number of data points for 2229 ADC pedestal subtraction.

8. The computer will show another box indicating that you should reconnect the ADC analog inputs.

[1] My present naming convention is `dtmmdd.log` where "`mmdd`" refer to the month and date of data collection. Most of this convention is not important. However, it is important to give the file the extension "`.log`".

[2] We are always referring to the top section of the 322G.

9. After reconnecting the inputs, put the logic unit in OFF mode.

10. Hit the "Done" button on the computer. The computer then does a calibration which takes about 5 minutes.

11. You will have to confirm the replacement of a file. The computer then takes data for FERA pedestal subtraction. You will know this is complete when a box comes up asking for confirmation to replace "pedestal.log."

12. At this point, the computer is trying to collect data. Turn on the high voltage to +2350 V and −2225 V. Also turn on the low voltage power supply.

13. Flip the logic unit to the AND position to trigger on coincidence of the scintillators.

Bibliography

[1] S.R. Amendolia. The spatial resolution of the ALEPH TPC. *Nuclear Instruments & Methods in Physics Research Section A*, 283:573–7, 1989.

[2] J. Baechler. Development of a TPC detector for the ALICE experiment. *Nuclear Instruments & Methods in Physics Research Section A*, 409:9–13, 1998.

[3] T. Behnke, S. Bertolucci, R.D. Heuer, and R. Settles. *TESLA, Technical Design Report*, chapter IV, pages 34–9. DESY, 2001.

[4] S.F. Biagi. Monte carlo simulation of electron drift and diffusion in counting gases under the influence of electric and magnetic fields. *Nuclear Instruments & Methods in Physics Research Section A*, 421(1–2):234–40, January 1999.

[5] C. Garabatos *et al.*. A TPC in the context of heavy-ion collisions. *Nuclear Instruments & Methods in Physics Research Section A*, 283:553–6, 1989.

[6] H. Aihara *et al.*. Spatial resolution of the PEP-4 time projection chamber. *IEEE Transactions on Nuclear Science*, NS-30(1):76–81, 1983.

[7] H. Wieman *et al.*. STAR TPC at RHIC. *IEEE Transactions on Nuclear Science*, 44:671–8, 1997.

[8] M.J. Berger *et al.*. Stopping-power and range tables for electrons, protons, and helium ions. *http://physics.nist.gov/PhysRefData/Star/Text/contents.html*, 2002.

[9] R. Itoh *et al.*. TOPAZ-TPC cosmic ray test. *IEEE Transactions on Nuclear Science*, NS-34(1):533–7, 1987.

[10] U. Becker *et al.*. The MIT LNS Drift Gases R&D Experiment. *http://cyclo.mit.edu/drift/*, 2002.

[11] LeCroy Corp. *Operator's Manual; Model 4300B CAMAC 16 channel Fast Encoding and Readout ADC (FERA)*, March 1998.

[12] William R. Leo. *Techniques for Nuclear and Particle Physics Experiments*, chapter 2, 6. Springer-Verlag, Berlin, 2nd edition, 1994.

[13] J. Marx and D. Nygren. The time projection chamber. *Physics Today*, 31(10):46–53, Oct 1978.

[14] A. Melissinos. *Experiments in Modern Physics*, chapter App. V, pages 544–5. Academic press, 1966.

[15] North American Working Group on Linear Collider Tracking. Revised baseline tracker designs (March 2001). http://www-mhp.physics.lsa.umich.edu/~keithr/LC/baselines_mar01.html.

[16] Y. Sacquin. The DELPHI time projection chamber. *Nuclear Instruments & Methods in Physics Research Section A*, 323:209–12, 1992.

[17] A. Sandstrom. *Cosmic Ray Physics*, chapter 1, pages 3–4, 43. North Holland Publishing Co., 1965.

[18] J. Wyatt. Signals with and without wires in modern detectors. Senior Thesis, Massachusetts Institute of Technology, 2001.